



Department of Precision and Microsystems Engineering

Reset Control for Vibration Isolation

Erdi Akyüz

Report no : 2018.035
Coach : Dr. S. H. HosseinNia & Dr. N. Saikumar
Professor : Ir. J.W. Spronck
Specialisation : Mechatronic System Design
Type of report : Master thesis
Date : October 31, 2018

Reset Control for Vibration Isolation

MASTER OF SCIENCE THESIS

For the degree of Master of Science in Mechanical Engineering at Delft
University of Technology

Erdi Akyüz

October 22, 2018

Faculty of Mechanical, Maritime and Materials Engineering (3mE) · Delft University of
Technology



Copyright © Precision and Microsystems Engineering
All rights reserved.

Abstract

Floor vibrations are a common problem in high tech engineering where good tracking, precision and bandwidth have utmost importance. They are mainly present at low frequencies, and they need to be suppressed. PID control is the go-to controller in the industry because of its ease of design, simple implementation and good performance. However, PID is subjected to the fundamental limitations of linear control theory - the waterbed effect and bode's gain-phase relationship. Therefore, it is not possible to improve one performance criterion, like stability, without negatively influencing the other. The need for overcoming the fundamental limitations of linear control initiates research towards nonlinear controllers.

Reset control is a type of nonlinear controller as a solution to overcome the limitations of a linear control. It reduces phase lag within the system, gives the advantage to reach higher bandwidth and results in lower overshoot or a faster settling time compared to linear controllers. However, using reset control comes with a price of unwanted dynamics due to the higher order harmonics. The main focus of this thesis is to improve disturbance rejection performance against floor vibrations by attenuating the power of high order harmonics. This problem has been tackled within the thesis, and a band-pass reset control is proposed.

Proposed reset controller applies reset only within the frequency range where floor vibrations are present, and it uses integrator as a reset variable. Results show reset controller that has a broadband phase compensation, like CgLp, is more advantageous towards phase lag reduction methods. CgLp is a reset element, which is an abbreviation of Constant-Gain Lead Phase. It gives broadband phase compensation within the desired range of frequencies by using generalized first order reset element. Also, CgLp controller achieved disturbance rejection performance of PI²D with the phase behavior of Clegg.

Table of Contents

Preface	vii
1 Introduction	1
2 Literature Review	3
3 Research Objective	11
3-1 Research Approach	11
3-2 Outline	11
4 Reset Control for Vibration Isolation	13
5 Conclusion	21
A Loop Shaping	23
B Loudspeaker Datasheet	25
C Detailed Setup Description	27
C-1 General Requirements	27
C-2 Conceptual Design	27
C-3 Detailed Setup	29
D BandPass Reset Control Analysis	32
D-1 HPF-LPF Option	32
E Current Amplifier V/A Ratio	37

List of Figures

1-1	High-tech instruments	1
1-2	Common sources of noise and vibration in a job environment. Image from LaserFocus.	2
A-1	A closed loop control system with process and output disturbance	23
C-1	Conceptual design of the setup.	28
C-2	Design concept no.1	28
C-3	Design concept no.2	29
C-4	Chosen design concept	29
C-5	Solidworks model of the finalized concept	30
C-6	Schematic overview of the experiment setup	30
C-7	Finalized setup. 1) Vibration source, 2) Actuator	31
D-1	Comparison between HPF-LPF option and state of the art controllers	33
D-2	Case IbHPF	34
D-3	Case IbLPF	35
D-4	Case HPFonly	35
D-5	Case LPFonly	36
E-1	Current Amplification rates	37

Preface

This thesis is made as a completion of the master of science in High-Tech Engineering(former PME).

Hereby, I would like to extend my sincere gratitude to everyone who contributed directly or indirectly to this thesis. I much appreciate Hassan HosseinNia and Niranjana Saikumar for their infinite source of patience and for their invaluable support during this process. I also want to thank Jo Spronck for encouraging me to think outside of the box.

I would like to thank my friends, my hidden heroes, both in Turkey and here for their psychological support. Who knew, a simple coffee break after spending endless times in a lab, struggling with bad results can keep a man sane and happy. Also, knowing the fact that I could reach my friends in Turkey anytime was a bliss.

Erdi Akyüz
Delft, October 2018

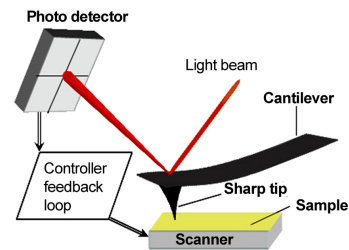
Chapter 1

Introduction

Tracking, precision, and bandwidth are three primary design objectives that require improvement as much as possible to excel in the market of high technology instruments. It is especially eminent in wafer scanners, which are machines used in the production of integrated circuits. To meet the demands of the high tech industry, the mass production of these microchips require nanometer accuracy and high-speed motion profiles [1]. Metrology applications such as atomic force microscopes and white light interferometers are also subjected to high-performance demands. Performance of these devices is affected by the external disturbances. Therefore, it is essential to have good disturbance rejection ability to reach the desired performance.



(a) A wafer scanner. Image taken from ASML.



(b) An atomic force microscopy representation.

Figure 1-1: High-tech instruments

Floor vibrations, an external disturbance, is ubiquitous in practice that vastly hinders the system performance. Although their intermittent character makes it impossible to model them in advance, they are present mainly at low frequencies (0.5-30 Hz) [2]. To reach nanometer accuracy, contactless positioning systems, such as air bearings, are used in the industry. For higher performance, next-generation precision positioning devices are designed to work in a vacuum environment [3]. This is so that they are less affected by floor vibrations. Besides these modifications, research has been conducted in feedback control systems to lessen a system's sensitivity against floor vibrations.

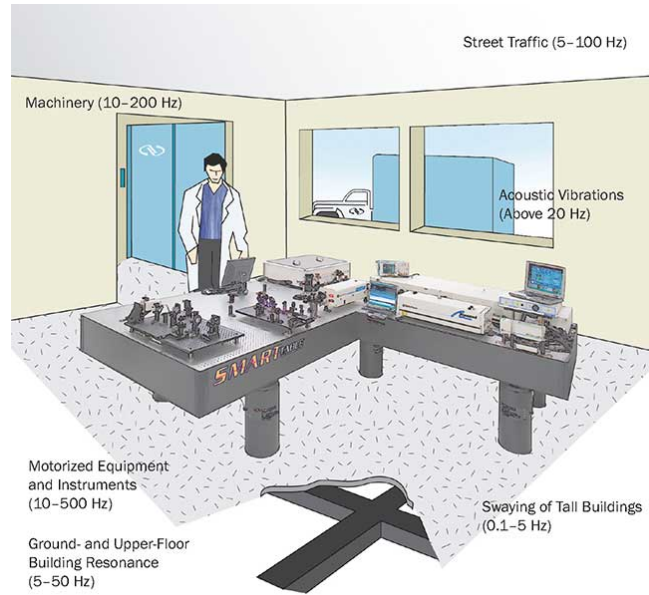


Figure 1-2: Common sources of noise and vibration in a job environment. Image from LaserFocus.

It is not a surprise that PID is widely being used in the industry due to its simple implementation and good performance regarding robustness and precision [4]. However, PID control is becoming insufficient as high precision positioning devices aim for nanometer accuracy. For this reason, two integrators are being used in the high tech industry, resulting in PI^2D [5]. Error minimization becomes higher at low frequencies due to the steeper gain slope compared to a single integrator. However, using a double integrator decreases the robustness of the system; thus a system with double integrator ends up having higher overshoot and settling time compared to a system with a single integrator.

Due to the fundamental limitations of linear control theory, it is not possible to increase disturbance rejection and robustness of a system at the same time. However, high tech industry requires a robust system good enough to nullify the disturbances and a system precise enough to reach desired positioning accuracy. As a result, the need for overcoming fundamental limitations of linear controllers initiate research towards nonlinear techniques such as reset control.

Reset control compensates the phase margin (PM) loss, or even increases the PM, reaches higher bandwidth, has less overshoot and a faster settling time compared to linear controllers [6]. However, there is a trade-off. Resetting a controller state introduces higher order harmonics into the system and creates unwanted dynamics. This is an important issue for precision positioning mechanisms where minimizing the error and reaching high accuracies are desired.

This issue is tackled in the literature. However, methods that have been used to circumvent this problem are either a trade-off between linear and reset control, or they were not useful concerning improving disturbance rejection. This thesis aims to improve disturbance rejection using reset control in a manner such that the effect of harmonics is minimized to not negatively affect other performance aspects.

Chapter 2

Literature Review

Chapter 2 consists of a literature review paper on disturbance rejection in reset systems. Reset strategies are investigated regarding disturbance rejection and the gap of this matter in the literature is shown.

A Review on Disturbance Rejection in Reset Systems

E. Akyüz, N. Saikumar, S. Hassan HosseinNia

Abstract—The high-tech industry has rigorous performance demands on tracking, precision, and bandwidth. The first two are, however, compromised by external disturbances. Therefore, disturbance rejection is a crucial factor in determining the performance. In the high-tech industry, where reaching utmost precision and robustness is necessary, PID control, which is dominantly used, is limited in the extent of disturbance rejection due to the fundamental limitations of a linear control such as Bode’s gain phase relationship and waterbed effect.

In literature, reset control has been used to overcome the limitations of linear control. However, few works exist from the point of view of disturbance rejection. Reset control also introduces high-order harmonics and can induce limit cycles and unwanted dynamics in the system.

This review paper concentrates on the work done in the reset control, particularly in improving disturbance rejection. Most popular existing reset strategies are analyzed from the disturbance rejection perspective.

I. INTRODUCTION

Tracking, precision, and bandwidth are three vital design objectives in high precision instruments. For example, wafer scanners, which are used in the production of integrated circuits, have to comply with stringent demands like nanometer precision and high-speed motion profiles. Tracking and precision performance, however, is negatively affected by external disturbances. Therefore, disturbance rejection performance is also crucial to meet the demands of the high-tech industry. Floor vibrations, an external disturbance, are ubiquitous in practice that vastly hinders the control performance. Although their intermittent character makes it impossible to model them in advance, they are present mainly at low frequencies (0.5-30 Hz), and they need to be suppressed [1].

PID control is widely used in the industry due to its simple implementation and good performance regarding robustness and precision [2]. However, PID is becoming insufficient to meet the performance criterion as the demands of the high-tech industry increase day by day. Disturbance rejection and robustness are conflicting terms in nature for linear controllers since it is impossible to improve one performance criterion without negatively influencing the other due to the waterbed effect. Waterbed effect states that improving disturbance rejection in one frequency range comes at the price of reduced disturbance rejection in another [3]. It can be seen clearly from Bode’s gain-phase relationship that increasing gain at low frequencies inevitably decreases the phase margin, thus compromising robustness. However, high tech industry requires a robust system capable of nullifying external disturbances sufficiently and precise enough to reach desired positioning accuracy. The need for overcoming fundamental limitations of linear

controllers has led to research into nonlinear controllers such as reset.

In 1958, Clegg [4] introduced a nonlinear integrator as a solution to surpass the limitations of a linear controller. He showed that this new nonlinear element, the so-called Clegg Integrator (CI), is able to lessen the overshoot and improve the stability by resetting the state of the integrator to zero whenever its input goes to zero (shown in Figure 1). He supported his claim with sinusoidal describing function analysis and showed that CI has 51.9° less phase lag at all frequencies while having gain characteristics 1.62 times more than the linear integrator (shown in Figure 2) [4]. Describing function of Clegg Integrator is described as:

$$CI(j\omega) = \frac{1.62}{j\omega} e^{j52^\circ} \quad (1)$$

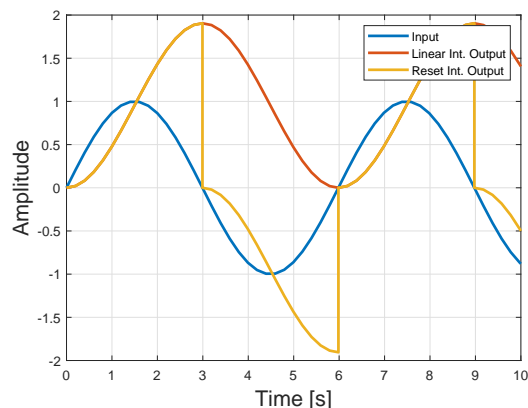


Fig. 1: Time response of Clegg integrator for a sinusoidal input

Later, Horowitz et al. extended the idea of Clegg and modified the Clegg Integrator by introducing the First Order Reset Element (FORE) [5] [6]. Hazeleger et al. [7] described Second Order Reset Element (SORE) and improved the design freedom compared to FOREs. More importantly, they attained improved disturbance rejection on an industrial stage system by increasing the bandwidth. On the other hand, Guo et al. [8] enhanced the design freedom of FORE by introducing an after reset control variable γ . This filter was termed Generalized FORE (GFORE). They pointed out that performance could be further improved by using nonzero reset matrices rather than applying conventional reset control. Finally, design flexibility

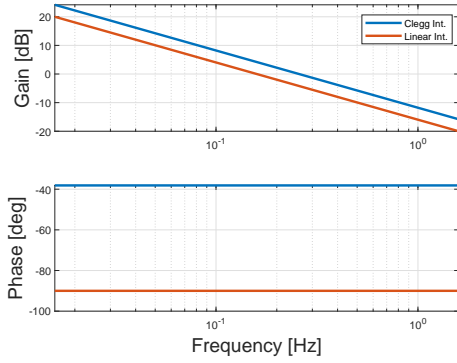


Fig. 2: Frequency response of Clegg integrator for a sinusoidal input

is improved to a higher extent with the introduction of fractional order dynamics to reset control [9] [10].

Reset control compensates the phase margin (PM) loss, or even increases the PM, reaches higher bandwidth, results in less overshoot or a faster settling time compared to linear controllers [11]. The main advantage of reset is that by using the describing function, reset controllers can be designed using loop shaping, which is the industry standard technique used for designing linear controllers, where the controller is designed by shaping the complete open loop (consisting of plant and controller) frequency response. However, using reset action introduces persisting oscillations or unwanted dynamics in the system response due to the introduction of higher order harmonics. While some methods to reduce the effect of these higher order harmonics exists, a comprehensive study of the most popular methods is necessary especially from the perspective of disturbance rejection.

This review paper is organized as follows. Section 2 describes the fundamental limitations of linear control with an example. Section 3 gives a general introduction of reset control. In this section, describing function is explained, followed by the introduction of Lyapunov stability analysis. Section 4 then gives an example to show the problem of using reset control and then introduces some of the existing reset strategies and analyses their disturbance rejection performance. Finally, Section 5 presents conclusions.

II. LIMITATION OF A LINEAR CONTROL

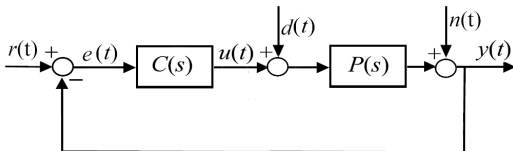


Fig. 3: A closed loop control system with disturbance

The general block diagram of a closed loop control system is shown in Figure 3 where $r(t)$ is reference, $y(t)$ is output,

$d(t)$ is process disturbance, $e(t)$ is error, $u(t)$ is control output, $n(t)$ is sensor noise, P is plant, and C is controller.

Disturbance rejection can be observed by looking at the process sensitivity (PS), which is the ratio of process disturbance to output (d to y) [3]. Lower PS means higher ability to reject disturbances. PS is described as: $PS = \frac{P}{1+PC}$. It is clear that controller gain must be increased to have higher disturbance rejection. Since we are mainly interested in rejecting disturbances at low frequencies, an option to increase the gain is through an integrator. However, an integrator creates phase lag, and this will reduce the phase margin and hence robustness of the system.

Consider a single mass-spring-damper plant and a PID controller with a low-pass filter. The transfer function of the plant is the following:

$$P(s) = \frac{1}{ms^2 + cs + k} \quad (2)$$

m, c, k denote mass, damping- and spring constant respectively. The plant parameters are chosen as 25 kg, 1114 N.m and 1e5 N/m respectively. Bandwidth is chosen as 100 Hz and the controller is tuned by using the rule of thumb [3]. As mentioned before, adding another integrator, creating PI²D, indeed increases the gain at low frequencies. However, from the open loop frequency response plot shown in Figure 4, it can be seen that the phase margin becomes lower with PI²D compared to PID. This trade-off can be explained by the Bode's gain-phase relationship.

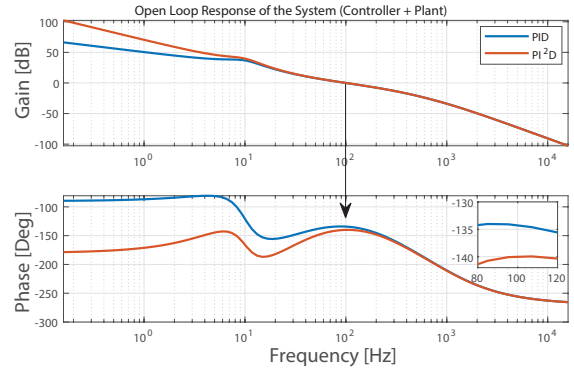


Fig. 4: Frequency response of open loop systems

Assume a 5 Hz sinusoidal process disturbance applied to the system. Figure 5 shows error signal of PID and PI²D respectively. The PI²D error is minimized due to higher gain at low-frequencies compared to PID control. However, due to the lower phase margin, the robustness of the system with PI²D is decreased. As a result, higher overshoot and settling time is observed compared to PID which can be seen in the unit step time response of the closed-loop system shown in Figure 6.

III. RESET CONTROL

A reset control system is a type of impulsive system that has a standard controller with a reset mechanism. This mechanism, in other words, switching surface provokes the control signal

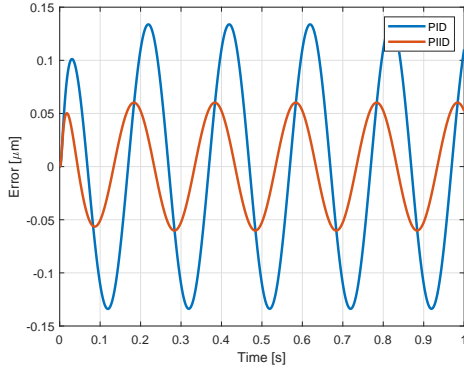


Fig. 5: 5 Hz sinusoidal input disturbance responses of closed loop systems

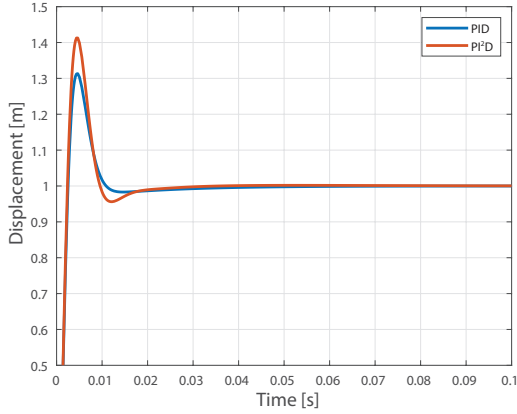


Fig. 6: Unit step time response of closed loop systems

to change when the system trajectory contacts this surface [12]. It is the reset action which overcomes the limitations of a linear controller. Reset element in Figure 7 shows that it requires two additional inputs apart from the error signal $e(t)$: One input $c(t)$ is required for determining the reset instants, in other words, reset condition. The remaining input $a(t)$ is used for defining the after reset value.

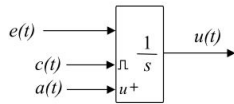


Fig. 7: Basic reset integrator with reset condition input $c(t)$ and after-reset value input $a(t)$. Image taken from [12]

Reset controller (Σ_R) as shown in Figure 8 consists of two parts: A base linear controller (C_b) whose states are not reset and a reset element (C) whose states are reset.

Open loop state space representation of reset controller and

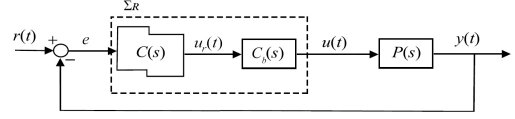


Fig. 8: Feedback loop with reset controller

the plant in series is given by

$$\begin{aligned} \dot{x} &= Ax + Be, & x, e, t &\notin \mathcal{M} \\ x(t^+) &= A_R x, & x, e, t &\in \mathcal{M} \\ y &= Cx + De \end{aligned}$$

where $x : [x_R^T, x_p^T]^T$ is the state vector of the open loop system where x_R and x_p denote reset controller and plant states respectively. $x_R(t) = [x_r^T, x_{nr}^T]^T$ where x_r and x_{nr} are states of the reset element (C) and base linear controller (C_b) respectively. The first and third equation of the state space representation is defined as flow mode where they show the continuous dynamic of the reset control system. Second equation, jump mode, introduces nonlinearity to the controller and activates when the reset condition is met. Finally, A_R determines the controller states to be reset and also their after reset value. $A_R = [A_\rho \ 0; 0 \ I]$ such that A_ρ has dimensions $n_r \times n_r$. The reset condition most popularly used in literature is zero crossing of the error input, i.e., $e(t) = 0$. In this paper, this is considered as the default for analysis.

A. Describing Function

Reset systems are nonlinear. A linear approximation technique called describing function (DF) is used in literature to study the frequency domain behaviour. DF is based on quasi-linearization. It means linearization depends on the form of the input signal [13]. Sinusoidal input is chosen as the input signal since ground vibrations show resemblance to the chosen input form.

Analytical calculation of DF of a general reset system is done by Guo et al. [8]. The following notation is defined for convenience:

$$\begin{aligned} \Lambda(\omega) &\triangleq \omega^2 + A^2 \\ \Delta(\omega) &\triangleq I + e^{\frac{\pi}{\omega} A} \\ \Delta_R(\omega) &\triangleq I + A_R e^{\frac{\pi}{\omega} A} \\ \Gamma_R(\omega) &= \Delta_R^{-1}(\omega) A_R \Delta(\omega) \Lambda^{-1}(\omega) \end{aligned}$$

By using the given notations, the sinusoid input describing function of the system found in [8] is:

$$G(j\omega) = C^T (j\omega I - A)^{-1} (I + j\Theta_D(\omega)) B + D \quad (3)$$

where

$$\Theta_D(\omega) \triangleq -\frac{2\omega^2}{\pi} \Delta(\omega) (\Gamma_R(\omega) - \Lambda^{-1}(\omega)) \quad (4)$$

Although DF gives an opportunity to examine the frequency response of the reset system, it is not completely accurate. The

main reason is that DF takes only first order harmonics of the nonlinear element and neglects the high order harmonics. Nuij et al. [14] introduced higher-order sinusoidal input describing functions (HOSIDFs) for nonlinear elements in general. Heinen analytically calculated HOSIDFs specifically for reset controllers. He showed the describing function as:

$$G(j\omega, n) = \begin{cases} C(j\omega I - A)^{-1}(I + j\Theta_D(\omega))B, & \text{for } n = 1 \\ \frac{-2\omega^2 C}{j\pi}(A - j\omega n I)^{-1}\Delta(\omega)[\Gamma_R(\omega) - \Lambda^{-1}(\omega)]B, & \text{for odd } n \geq 2 \\ 0, & \text{for even } n \geq 2 \end{cases} \quad (5)$$

where n denotes the order of the harmonics [15]. Based on the given equation, higher order harmonics can be plotted. Figure 9 shows the frequency behavior of Clegg integrator with harmonics up-to 13th order plotted. This provides us with a useful tool to more accurately understand the performance of reset control systems and the effect that the harmonics have on overall system performance.

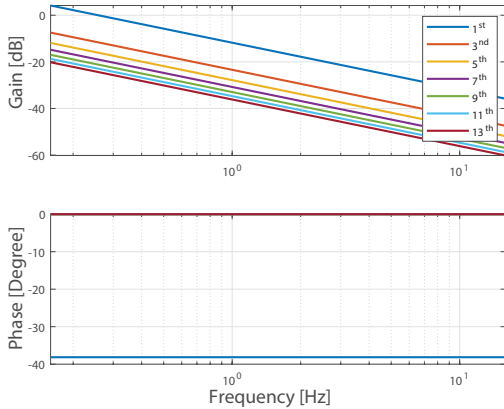


Fig. 9: Clegg integrator (shown in blue) and its higher order harmonics up to 13th order

B. Lyapunov Stability Analysis

Consider reset controller (Σ_R) in a closed loop with a plant as shown in Figure 8. The following conditions must be satisfied to have asymptotic stability:

Theorem 1: [12] Let $V: \mathbb{R}^n \rightarrow \mathbb{R}$ be a continuously differentiable, positive-definite, radially unbounded function such that

$$\dot{V}(\mathbf{x}) := \left(\frac{\partial V}{\partial \mathbf{x}} \right)^T A_{cl} \mathbf{x} < 0, \quad \text{for } \mathbf{x} \neq 0 \quad (6)$$

$$\Delta V(\mathbf{x}) := V(A_R \mathbf{x}) - V(\mathbf{x}) \leq 0, \quad \text{for } \mathbf{x} \in \mathcal{M} \quad (7)$$

Then the reset control system is asymptotically stable.

where A_{cl} and A_R denote closed loop A-matrix and reset matrix respectively. $\mathbf{x} = [x_R^T \ x_p^T]^T$ represents the state

vector. For quadratic stability of the system, (6) and (7) must satisfy the function $V(\mathbf{x}) = \mathbf{x}^T P \mathbf{x}$ with $P > 0$. Following proposition will suffice for proving quadratic stability:

Theorem 2: [12] There exists a constant $\beta \in \mathcal{R}^{n_r \times 1}$ and $P_\rho \in \mathcal{R}^{n_r \times n_r}$ such that the restricted Lyapunov equation

$$P > 0, \quad A_{cl}^T P + P A_{cl} < 0, \quad (8)$$

$$B_0^T P = C_0 \quad (9)$$

has a solution for P . The matrices B_0 and C_0 are defined as

$$C_0 = (P_\rho \ 0_{n_r \times n_{nr}} \ \beta C_p), \quad B_0 = \begin{pmatrix} I_{n_r \times n_r} \\ 0_{n_{nr} \times n_r} \\ 0_{n_r \times n_r} \end{pmatrix} \quad (10)$$

where C_p is $1 \times n_p$ and n_p is the number of plant states.

IV. EXISTING RESET STRATEGIES FOR DISTURBANCE REJECTION

PI²D control has a higher gain at low frequencies compared to PID control. Therefore, it has better disturbance rejection at low frequencies. However, as noted in section 2, PI²D control is less robust than PID due to the lower phase margin. In literature, one of the integrators of PI²D is replaced by a Clegg Integrator, making PI(Cl)D. PI(Cl)D results in a reduction of phase lag and hence results in increased phase margin even higher than PID. Thus, a more robust controller than PI²D with better disturbance rejection performance than PID is expected. However, this is not true.

Reset integrators do not have the same steady-state error characteristics as linear integrators. As shown in Figure 10, high-order harmonics result in unwanted dynamics in closed loop system performance. Furthermore, they introduce undesired spikes under disturbance. Consider a 5 Hz sinusoidal process disturbance applied to the system. Figure 11 shows the error signal of PI²D and PI(Cl)D respectively. Undesired spikes are observed in the error signal of the system with PI(Cl)D controller due to the high-order harmonics. These spikes significantly deteriorate the performance of the high precision systems.

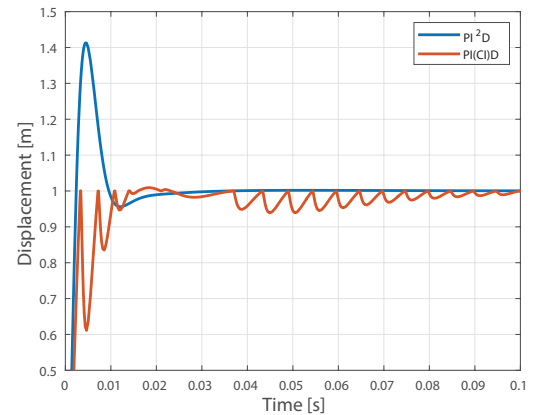


Fig. 10: Unit step response of closed loop systems

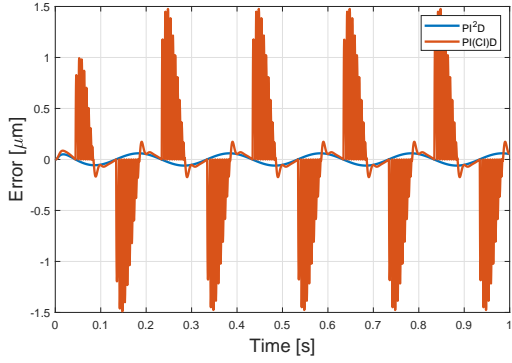


Fig. 11: 5 Hz sinusoidal input disturbance responses of closed loop systems

Reset strategies studied in literature have mainly been for performance improvement without taking into account the negative effects of high-order harmonics. Furthermore, only a few works exist for disturbance rejection improvement. Following reset strategies are proposed in the existing literature:

A. Partial Reset

Consider the reset matrix $A_\rho = \gamma I$, where γ is a scalar value between 0 and 1. The behavior of reset controller changes with the gamma value: $\gamma = 1$ for no reset and $\gamma = 0$ for traditional reset. However, it is also possible to introduce a partial reset by choosing a γ value between 0 and 1. As the value of gamma gets closer to one, the phase advantage reduces along with a reduction in the higher order harmonics.

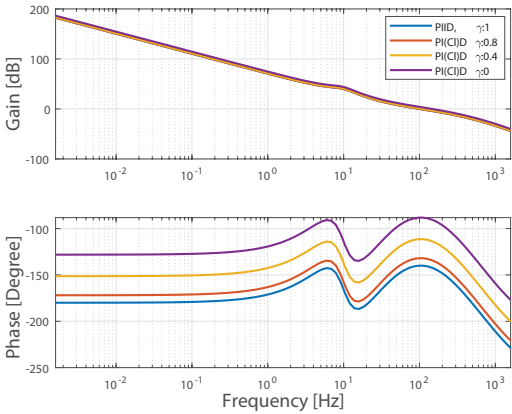


Fig. 12: Describing function of the open loop system with various γ values

Partial reset allows to reach optimum overshoot/undershoot value as shown in Figure 13. As the γ value is chosen closer to 1, maximum error decreases as shown in Figure 14. However, it cannot improve the disturbance response compared to the linear controller. Rather, partial reset only provides a trade-off between limit cycles and phase advantage of reset.

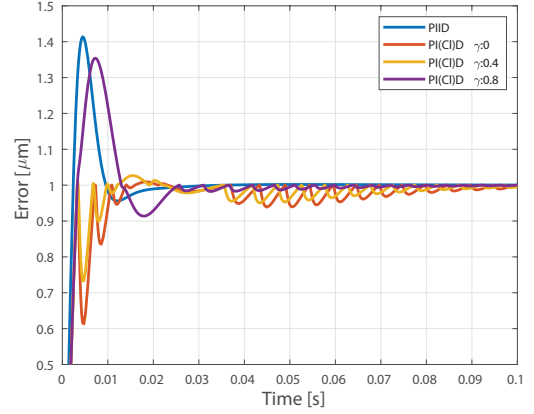


Fig. 13: Unit step response in time domain

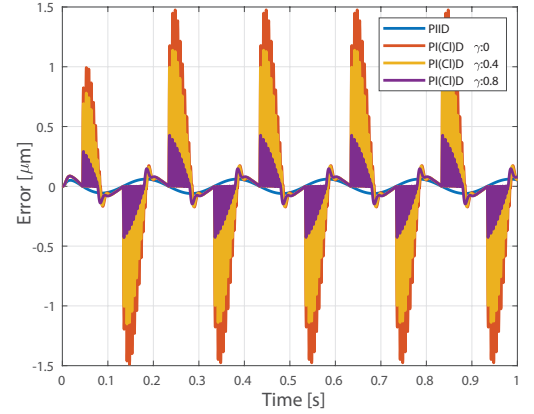


Fig. 14: 5 Hz sine input disturbance response

B. Reset Band

In conventional reset controllers, reset condition is triggered at zero crossing of the error input. However, in reset systems with reset band, reset instants are determined by reset lines [16]. Reset band surface B_δ defined with the reset lines is given by $B_\delta = \{(x, y) \in \mathbf{R}^2 | (x = -\delta \wedge y > 0) \vee (x = \delta \wedge y < 0)\}$

The parameter δ defines the type of the controller. Conventional reset control is obtained if $\delta = 0$. Whereas linear control is achieved if the ratio of δ to the error amplitude is big. Vidal et al. [17] noted that using reset band is advantageous towards time-delay systems. They showed that selecting a wide reset band can eliminate the limit cycles as well. However, Ivens in [18] shows that limit cycles can occur even with this modification in some systems.

Regarding improving disturbance rejection against floor vibrations, reset band method is not advantageous, because the controller loses its robustness against disturbances as the range of reset band increases. Within the reset band, controller behaves as a linear controller and hence the advantage of reset is lost. Furthermore, no specific literature exists to determine

what the reset band should be for a given plant. Then, reset becomes impractical.

C. Time Regularization

In general, reset mechanism of reset control system is only state-dependent and independent of time. However, reset mechanism can also be time-dependent or both time-dependent and state-dependent.

Time-dependent reset mechanisms require predefined fixed reset instants. It is problematic to find reset time intervals where the system is subjected to ground vibrations since, these instants are not well studied and no method exists to obtain them in the literature yet.

D. Reset Ratio (PI+CL Controller)

Reset ratio, $p_{reset} \in [0, 1]$, is another tuning parameter that is being used particularly in PI+CI controllers. As the controller structure is shown in Figure 15, integrator and Clegg integrator are combined in parallel. p_{reset} determines the weightage given to the reset controller part. Reset is eliminated if $p_{reset} = 0$. On the other hand, linear integrator is eliminated if $p_{reset} = 1$. When $p_{reset} \in (0, 1)$, steady-state error could be eliminated by linear integrator and the transient response of the system could be improved by CI term.

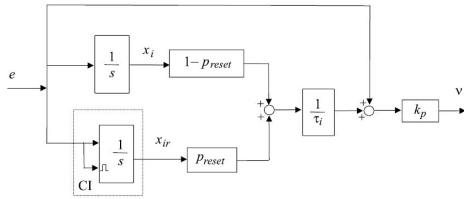


Fig. 15: Block diagram representation of PI+CI [12]

It has been shown that resetting a percentage of the integral term improves the settling time and reduces the overshoot significantly [19]. Vidal and Banos [20] extended the performance of PI+CI by introducing a variable reset ratio instead of a fixed reset ratio. However, it is important to note that reset ratio introduces trade-off between linear and reset control.

E. Application

In the existing literature, researchers improved disturbance rejection as a consequence of improving bandwidth with reset control. The only application solely for improved disturbance rejection is made by Li et al. [21] in Hard Disk Drives. In [21], PI lead controller is designed to stabilize the servo loop and notch filter is used to remove high-frequency harmonics. They achieved 50% higher midfrequency disturbance rejection compared to linear control. By using reset control, they achieved phase advantage at desired frequencies without influencing the gain characteristic. However, they achieved narrowband disturbance rejection which is insufficient for floor vibrations.

V. CONCLUSION

The literature review has shown that while reset control has been extensively used to improve stability and some performance aspects, researchers mainly focused on eliminating the limit cycles, on decreasing the overshoot and settling time of the chosen system. Disturbance rejection performance is mainly increased by increasing the bandwidth. Unfortunately, research towards disturbance rejection at low-frequencies is lacking. Furthermore, there exists a gap in removing the negative effects of the high-order harmonics in terms of disturbance rejection in the literature.

Reset methods are investigated and it has been shown that partial reset, reset band, time regularization and reset ratio are the four possible methods known in the literature to improve the performance of a reset control. Researchers have showed fixed/variable reset band improves the performance. However, it is not the recommended method when uncertainties are present. For the same reason, fixed time instant is not a suitable method against uncertainties since they can cause instabilities. PI+CI is widely used in the literature. Unfortunately, it merely provides a trade-off between linear and reset control.

Based on the studied literature, it appears that improved disturbance rejection using reset control against low-frequency range vibrations requires more attention.

REFERENCES

- [1] S. Ryan, "Optical table advances quiet vibrations in highly sensitive applications," *LASER FOCUS WORLD*, vol. 53, no. 9, pp. 27–30, 2017.
- [2] K. J. Astrom and T. Hagglund, "The future of PID control," *Control Engineering Practice*, vol. 9, no. 11, pp. 1163–1175, 2001.
- [3] R. M. Schmidt, G. Schitter, and A. Rankers, *The Design of High Performance Mechatronics: High-Tech Functionality by Multidisciplinary System Integration*. IOS Press, 2014.
- [4] J. C. Clegg, "A nonlinear integrator for servomechanisms," *Transactions of the American Institute of Electrical Engineers, Part II: Applications and Industry*, vol. 77, no. 1, pp. 41–42, 1958. [Online]. Available: <http://ieeexplore.ieee.org/document/6367399/>
- [5] I. Horowitz and P. Rosenbaum, "Non-linear design for cost of feedback reduction in systems with large parameter uncertainty," *International Journal of Control*, vol. 21, no. 6, pp. 977–1001, 1975.
- [6] K. Krishnan and I. Horowitz, "Synthesis of a non-linear feedback system with significant plant-ignorance for prescribed time-domain tolerances," 1973.
- [7] L. Hazeleger, M. Heertjes, and H. Nijmeijer, "Second-order reset elements for stage control design," *Proceedings of the American Control Conference*, vol. 2016-July, pp. 2643–2648, 2016.
- [8] Y. Guo, Y. Wang, and L. Xie, "Frequency-domain properties of reset systems with application in hard-disk-drive systems," *IEEE Transactions on Control Systems Technology*, vol. 17, no. 6, pp. 1446–1453, 2009.
- [9] S. H. Hosseinnia, I. Tejado, D. Torres, B. M. Vinagre, and V. Feliu, "A general form for reset control including fractional order dynamics," *IFAC Proceedings Volumes (IFAC-PapersOnline)*, vol. 19, no. i, pp. 2028–2033, 2014.
- [10] N. Saikumar, H. Hosseinnia, and M. Engineering, "Generalized Fractional Order Reset Element (GFrORE)," vol. 2, no. 1, 2017.
- [11] O. Beker, C. V. Hollot, Y. Chait, and H. Han, "Fundamental properties of reset control systems," *IFAC Proceedings Volumes (IFAC-PapersOnline)*, vol. 15, no. 1, pp. 187–192, 2002.
- [12] A. Baños and A. Barreiro, *Reset Control Systems*, ser. Advances in Industrial Control. London: Springer London, 2012. [Online]. Available: <http://www.springer.com/engineering/control/book/978-0-85729-634-4http://link.springer.com/10.1007/978-1-4471-2250-0>
- [13] W. E. Vander Velde, *Multiple-input describing functions and nonlinear system design*. McGraw-Hill, New York, 1968.

- [14] P. Nuij, O. Bosgra, and M. Steinbuch, "Higher-order sinusoidal input describing functions for the analysis of non-linear systems with harmonic responses," *Mechanical Systems and Signal Processing*, vol. 20, no. 8, pp. 1883 – 1904, 2006. [Online]. Available: <http://www.sciencedirect.com/science/article/pii/S088832700500083X>
- [15] K. Heinen, "Frequency analysis of reset systems ." [Online]. Available: <http://dx.doi.org/10.1016/j.sysconle.2013.10.002>
- [16] A. Barreiro, A. Baños, S. Dormido, and J. A. González-Prieto, "Reset control systems with reset band: Well-posedness, limit cycles and stability analysis," *Systems and Control Letters*, vol. 63, no. 1, pp. 1–11, 2014. [Online]. Available: <http://dx.doi.org/10.1016/j.sysconle.2013.10.002>
- [17] A. Vidal and A. Banos, "QFT-based design of PI+ CI reset compensators: application in process control," *Control and Automation, 2008 16th ...*, pp. 806–811, 2008. [Online]. Available: http://ieeexplore.ieee.org/xpls/abs/_all.jsp?arnumber=4602123
- [18] M. Ivens, "Robust reset control," 2017. [Online]. Available: <http://dx.doi.org/10.1016/j.sysconle.2013.10.002>
- [19] A. Banos and A. Vidal, "Design of Reset Control Systems: The PI + CI Compensator," *Journal of Dynamic Systems, Measurement, and Control*, vol. 134, no. 5, p. 051003, 2012. [Online]. Available: <http://dynamicsystems.asmedigitalcollection.asme.org/article.aspx?articleid=1478002>
- [20] A. Vidal and A. Banos, "Stability of reset control systems with variable reset: Application to pi+ ci compensation," in *Control Conference (ECC), 2009 European*. IEEE, 2009, pp. 4871–4876.
- [21] Y. Li, G. Guo, and Y. Wang, "Reset control for midfrequency narrow-band disturbance rejection with an application in hard disk drives," *IEEE Transactions on Control Systems Technology*, vol. 19, no. 6, pp. 1339–1348, 2011.

Research Objective

Literature review of reset systems with respect to disturbance rejection is given in chapter 2. From the literature review paper, it is seen that low-frequency range vibrations require more attention in terms of disturbance rejection. Based on this conclusion, research objective of this thesis is set:

Improve the disturbance rejection performance of reset systems against floor vibrations by attenuating the presence of high order harmonics within the region of interest.

3-1 Research Approach

Following research approach is adopted to reach the objective:

- Explore novel reset control strategies to suppress floor vibration by improving the disturbance rejection performance.
- Analyze the proposed method theoretically and in simulations respectively.
- Validate the novel method experimentally by implementing it on position locking setup.

3-2 Outline

This master thesis is organized as follows: Chapter 2 has described the existing reset strategies available in the state of art. Their advantages and disadvantages are investigated with respect to disturbance rejection performance. In Chapter 4, new reset controller designs are presented and their performance is analyzed. Next, the results and conclusions of chapter 4 are thoroughly discussed in the final chapter.

Chapter 4

Reset Control for Vibration Isolation

Chapter 4 is presented in a conference paper format. Disturbance rejection through reset is investigated. The aim of this paper is to show how disturbance rejection can be improved by attenuating the high-order harmonics in reset systems.

Reset Control for Vibration Isolation

Erdi Akyüz

Abstract—High speeds and accelerations with nanometer accuracy are a necessity to meet the demands of the high tech industry. However, immediate attention is needed towards rejecting floor vibrations, since they greatly affect the system performance. PID control is widely used in the industry to have good disturbance rejection. But, it is affected by Bode's gain phase relationship and waterbed effect. Reset control is a promising method to surpass the limitations of a linear controller. However, they are limited regarding disturbance rejection performance due to the controller introduced higher order harmonics that induces unwanted dynamics into the system. This paper aims to improve disturbance rejection through reset by looking at two different strategies to reduce higher order harmonics namely phase lag reduction and phase compensation. Band-pass reset control is proposed to overcome the negative effects that cause performance degradation as a phase reduction method. Results show phase compensation around the bandwidth is advantageous compared to phase reduction methods.

I. INTRODUCTION

Tracking, precision, and bandwidth are three primary design objectives that require constant improvement to excel in the market of high technology instruments. It is especially eminent in wafer scanners, which are machines used in the production of integrated circuits. To meet the demands of the high tech industry, these machines require nanometer accuracy and high-speed motion profiles [1]. Metrology applications such as atomic force microscopes and white light interferometers are also subjected to high-performance demands. The performance of these devices, however, is also affected by the external disturbances. Therefore, it is essential to have good disturbance rejection ability to reach the desired performance.

Floor vibrations, an external disturbance, is ubiquitous in practice that vastly hinders the system performance. Although their intermittent character makes it impossible to model them in advance, they are present mainly at low frequencies (0.5-30 Hz) [2]. To reach nanometer accuracy, contactless positioning systems, such as air bearings, are used in the industry. For higher performance, next-generation precision positioning devices are designed to work in a vacuum environment [3]. Besides these modifications, research has been conducted in feedback control systems to lessen a system's sensitivity against floor vibrations.

PID is widely used in the industry due to its simple implementation and good performance concerning robustness and precision [4]. However, PID control is becoming insufficient as high precision positioning devices aim for higher bandwidths and higher precisions. In order to have nanometer accuracy, double integrators are used in the high tech industry [5]. Error minimization becomes higher at low frequencies

due to the steeper gain slope compared to a single integrator. However, using a double integrator decreases the robustness of the system. Thus, a system with double integrator ends up having higher overshoot and settling time compared to a system with a single integrator.

Disturbance rejection and robustness are conflicting terms in nature for linear controllers since it is impossible to improve one performance criterion without negatively influencing the other due to the waterbed effect. Waterbed effect states that improving the disturbance rejection performance of a system in a particular frequency range will inevitably reduce the disturbance rejection in other regions [6]. It can be seen clearly from Bode's gain-phase relationship that increasing gain at low frequencies inevitably decreases the phase margin, thus compromising robustness. However, high tech industry requires a robust system capable of nullifying external disturbances sufficiently and precise enough to reach desired positioning accuracy. The need for overcoming fundamental limitations of linear controllers has led to research into nonlinear controllers such as reset.

In 1958, a nonlinear type of integrator was proposed by Clegg to overcome the aforementioned limitations of a linear controller [7]. He claimed that this new nonlinear element, the so-called Clegg Integrator (CI), can provide lower overshoot and thus improves the stability. Clegg integrator switches from continuous to jump state when error input goes to zero. An advantage of Clegg integrator is that it provides 51.9° less phase lag at all frequencies while having gain characteristics 1.62 times higher than the linear integrator [7].

Researchers improved disturbance rejection as a consequence of improving bandwidth with reset control. The only application solely for improved disturbance rejection is made by Li et al. in Hard Disk Drives. They achieved 50% higher midfrequency disturbance rejection compared to linear control by implementing reset control [8].

Using reset control, however, causes unwanted dynamics in the closed loop response due to the high-order harmonics. Furthermore, undesired spikes are introduced under disturbances. These spikes deteriorate the performance of the high precision systems.

In the existing literature, there are some methods to compensate for this problem. These methods are partial reset, PI+CI [9], [10], reset band [11], and time regularization [12] respectively. Although the existing literature has solutions for this problem, they are either a trade-off between linear and reset control or ineffective regarding improving disturbance rejection. More importantly, no work is done on attenuating the negative effects of high order harmonics. Hence, research

to improve disturbance rejection is needed.

This research paper is organized as follows. Section 2 gives preliminary information about reset control. Section 3 introduces two approaches to improve disturbance rejection performance. Then, system design is explained in Section 4. In this section, the experimental setup is explained, followed by the system identification. Section 5 gives the experimental verification. Finally, Section 6 presents conclusions.

II. PRELIMINARY

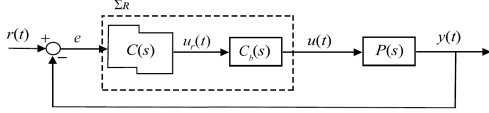


Fig. 1. Feedback loop with reset controller

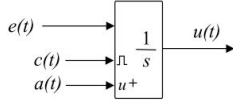


Fig. 2. Basic reset integrator with reset condition input $c(t)$ and after-reset value input $a(t)$. Image taken from [13]

A. Reset Control

A reset control system is a type of impulsive system that has a standard controller with a reset mechanism. This mechanism, in other words, switching surface provokes the control signal to change when the system trajectory contacts this surface [13]. It is the reset action which overcomes the limitations of a linear controller. Reset element in Figure 2 shows that it requires two additional inputs apart from the error signal $e(t)$: One input $c(t)$ is required for determining the reset instants, in other words, reset condition. The remaining input $a(t)$ is used for defining the after reset value.

Reset controller (Σ_R) as shown in Figure 1 consists of two parts: A base linear controller (C_b) whose states are not reset and a reset element (C) whose states are reset.

Open loop state space representation of reset controller and the plant in series is given by

$$\begin{aligned} \dot{x} &= Ax + Be, & x, e, t &\notin \mathcal{M} \\ x(t^+) &= A_R x, & x, e, t &\in \mathcal{M} \\ y &= Cx + De \end{aligned}$$

where $x : [x_R^T, x_p^T]^T$ is the state vector of the open loop system where x_R and x_p denote reset controller and plant states respectively. $x_R(t) = [x_r^T, x_{nr}^T]^T$ where x_r and x_{nr} are states of the reset element (C) and base linear controller (C_b) respectively. The first and third equation of the state space representation is defined as flow mode where they show the continuous dynamic of the reset control system. Second equation, jump mode, introduces nonlinearity to the controller and activates when the reset condition is met.

Finally, A_R determines the controller states to be reset and also their after reset value. $A_R = [A_p \ 0; 0 \ I]$ such that A_p has dimensions $n_r \times n_r$. In this paper, reset condition is set as zero crossing of the error input, i.e., $e(t) = 0$.

B. Describing Function

Reset systems are nonlinear. A linear approximation technique called describing function is used in literature to study the frequency domain behaviour. DF is based on quasi-linearization. It means linearization depends on the form of the input signal [14]. Sinusoidal input is chosen as the input signal since ground vibrations show resemblance to the chosen input form.

Analytical calculation of DF of a general reset system is done by Guo et al. [15]. The following notation is defined for convenience:

$$\begin{aligned} \Lambda(\omega) &\triangleq \omega^2 + A^2 \\ \Delta(\omega) &\triangleq I + e^{\frac{\pi}{\omega} A} \\ \Delta_R(\omega) &\triangleq I + A_R e^{\frac{\pi}{\omega} A} \\ \Gamma_R(\omega) &= \Delta_R^{-1}(\omega) A_R \Delta(\omega) \Lambda^{-1}(\omega) \end{aligned}$$

By using the given notations, the sinusoid input describing function of the system found in [15] is:

$$G(j\omega) = C^T (j\omega I - A)^{-1} (I + j\Theta_D(\omega)) B + D \quad (1)$$

where

$$\Theta_D(\omega) \triangleq -\frac{2\omega^2}{\pi} \Delta(\omega) (\Gamma_R(\omega) - \Lambda^{-1}(\omega)) \quad (2)$$

Although DF gives an opportunity to examine the frequency response of the reset system, it is not completely accurate. The main reason is that DF takes only first order harmonics of the nonlinear element and neglects the high order harmonics. Nuij et al. [16] introduced higher-order sinusoidal input describing functions (HOSIDFs) for nonlinear elements in general. Heinen analytically calculated HOSIDFs specifically for reset controllers. He showed the describing function as:

$$G(j\omega, n) = \begin{cases} C(j\omega I - A)^{-1} (I + j\Theta_D(\omega)) B, & \text{for } n = 1 \\ \frac{-2\omega^2 C}{j\pi} (A - j\omega I)^{-1} \Delta(\omega) [\Gamma_R(\omega) - \Lambda^{-1}(\omega)] B, & \text{for odd } n \geq 2 \\ 0, & \text{for even } n \geq 2 \end{cases} \quad (3)$$

where n denotes the order of the harmonics [17]. Based on the given equation, higher order harmonics can be plotted. Figure 3 shows the frequency behavior of Clegg integrator with harmonics up-to 5th order plotted. This provides us with a useful tool to more accurately understand the performance of reset control systems and the effect that the harmonics have on overall system performance.

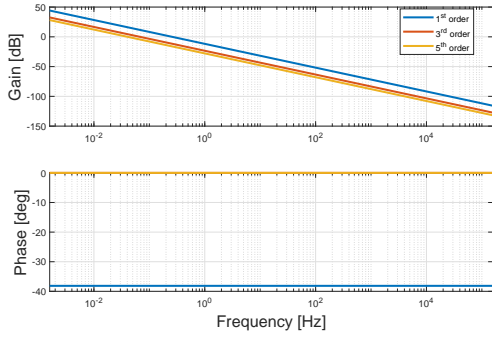


Fig. 3. Frequency behavior of Clegg integrator including high order harmonics

C. Lyapunov Stability Analysis

Consider reset controller (Σ_R) in a closed loop with a plant as shown in Figure 1. The following conditions must be satisfied to have asymptotic stability:

Theorem 1: [13] Let $V: \mathbb{R}^n \rightarrow \mathbb{R}$ be a continuously differentiable, positive-definite, radially unbounded function such that

$$\dot{V}(\mathbf{x}) := \left(\frac{\partial V}{\partial \mathbf{x}} \right)^T A_{cl} \mathbf{x} < 0, \quad \text{for } \mathbf{x} \neq 0 \quad (4)$$

$$\Delta V(\mathbf{x}) := V(A_R \mathbf{x}) - V(\mathbf{x}) \leq 0, \quad \text{for } \mathbf{x} \in \mathcal{M} \quad (5)$$

Then the reset control system is asymptotically stable.

where A_{cl} and A_R denote closed loop A-matrix and reset matrix respectively. $\mathbf{x} = [x_R^T \ x_p^T]^T$ represents the state vector. For quadratic stability of the system, (4) and (5) must satisfy the function $V(\mathbf{x}) = \mathbf{x}^T P \mathbf{x}$ with $P > 0$. Following proposition will suffice for proving quadratic stability:

Theorem 2: [13] There exists a constant $\beta \in \mathbb{R}^{n_r \times 1}$ and $P_\rho \in \mathbb{R}^{n_r \times n_r}$ such that the restricted Lyapunov equation

$$P > 0, \quad A_{cl}^T P + P A_{cl} < 0, \quad (6)$$

$$B_0^T P = C_0 \quad (7)$$

has a solution for P . The matrices B_0 and C_0 are defined as

$$C_0 = (P_\rho \ 0_{n_r \times n_r} \ \beta C_p), \quad B_0 = \begin{pmatrix} I_{n_r \times n_r} \\ 0_{n_r \times n_r} \\ 0_{n_r \times n_r} \end{pmatrix} \quad (8)$$

where C_p is $1 \times n_p$ and n_p is the number of plant states.

III. RESET CONTROL FOR VIBRATION ISOLATION

As mentioned in the introduction section, floor vibrations are in the frequency range of 0.5 to 30 Hz and PI²D control is used in practice to reach higher disturbance rejection. However, its performance is limited due to the fundamental limitations of a linear controller. Research has been done in reset to overcome these limitations. There are two ways to use reset: 1) phase lag reduction and 2) phase compensation.

A. Phase Lag Reduction

In this method, reset action is introduced to one of the phase lag introducing filters in the base linear controller. In most literature, integrator is chosen. For example, if one of the integrators of PI²D is replaced with Clegg integrator (PI(CI)D), phase lag will be reduced from 180 degrees to around 128 degrees. As a result, the phase margin of the system increases. However, resetting action also introduces high order harmonics and can degrade performance. This can be seen in the response of a mass spring damper system to a 5 Hz sinusoidal disturbance in Figure 4 compared with that of PI²D.

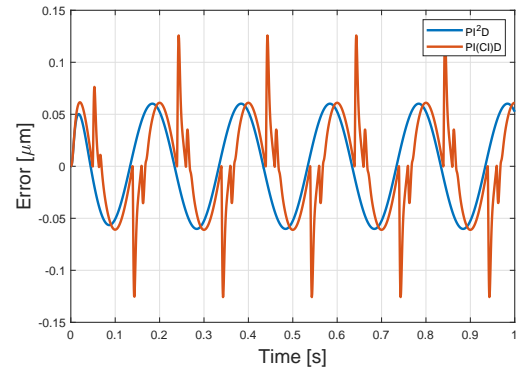


Fig. 4. 5 Hz sinusoidal input disturbance responses of closed loop systems

Figure 3 shows first, third and fifth harmonics of a Clegg integrator, created by HOSIDFs. It can be seen that magnitude of high order harmonics are not negligible compared to the first harmonic at all frequencies. It could be hypothesized that the attenuation of these harmonics in the required frequency range will result in improved performance. In this case, since we are interested in disturbance rejection in a frequency range, we propose a band-pass reset approach to verify this hypothesis.

Band-pass reset action is created using a high-pass filter and a low-pass filter. If they have same cut-off frequency, ω_b , their transfer functions are:

$$HPF = \frac{s}{\omega_b + s} \quad LPF = \frac{\omega_b}{\omega_b + s} \quad (9)$$

Summation of these filters gives static gain. If a PI ($1+wi/s$) is introduced before these filters, then the result will be a PI filter as shown in the following equation.

$$\left(1 + \frac{\omega_i}{s}\right) .HPF + \left(1 + \frac{\omega_i}{s}\right) .LPF = \left(1 + \frac{\omega_i}{s}\right) \quad (10)$$

This provides 4 possible states (2 in each parallel branch) which can be considered for reset as shown in Figure 5. PCI can be formed if both integrators are reset. However, if only one of the integrators is reset, then reset action and its corresponding frequency behavior can be seen either before or after ω_b .

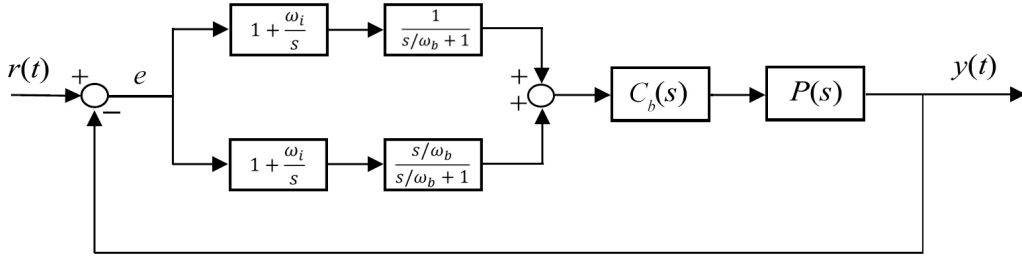


Fig. 5. Band-Pass control block diagram

In this paper, CI in PI(CI)D controller is substituted with the band-pass reset control. Figure 5 shows the block diagram representation of band-pass reset control. One of the integrator has now the band-pass configuration. The second integrator remains in the base linear controller, C_b . Four different controller configurations is achieved by resetting one of the four possible elements of the band-pass architecture. Comparison is made by tuning the first harmonic open loop responses in such a way that they give same gain response.

Abbreviations in figures are:

- IbHPF: Resetting Integrator before the HPF
- IbLPF: Resetting Integrator before the LPF
- HPF: Resetting only HPF
- LPF: Resetting only LPF

B. Phase Compensation

While reset has mainly been used for phase lag reduction in literature, Saikumar et al. showed in [18] that broadband phase compensation could be achieved with reset through the design of their CgLp element. With CgLp filter, a reset lag filter is used in series with a linear lead filter to achieve unity gain but with phase lead in the desired frequency range.

The disadvantage of PI²D over PID is the reduced phase margin although the gain at low frequencies is as desired. This loss in phase at bandwidth can be compensated for using the CgLp element. Further, since the CgLp filter can be designed to provide phase in the desired frequency range, high order harmonics introduced by the resetting action will also be restricted to a range of frequencies.

The design of CgLp element is provided as:

$$R = \frac{1}{s/\omega_{r\alpha} + 1} \quad \text{and} \quad L = \frac{s/\omega_r + 1}{s/\omega_f + 1} \quad (11)$$

where R and L denote first order lag filter reset and first order lead filter respectively, This CgLp filter provides phase compensation mainly in the range $[\omega_r, \omega_f]$, where ω_r , $\omega_{r\alpha}$ and ω_f are cut-off frequency of CgLp, ω_r with a correction factor and low-pass filter respectively. Also, condition $\omega_f \gg \omega_{r\alpha}, \omega_r$ must hold. Correction factor in $\omega_{r\alpha}$ is chosen as mentioned in [18]. A positive phase is achieved with this filter even beyond this range. This CgLp filter is used in series with the PI²D, which acts as the base linear controller.

The value ω_r is chosen in a way that it has a phase margin similar to PI(CI)D.

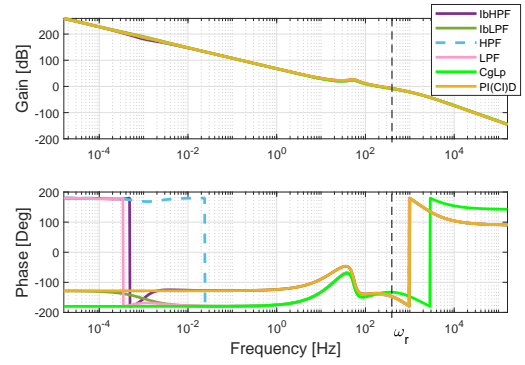


Fig. 6. 1st order harmonics of possible reset variables of band-pass and CgLp using HOSIDFs

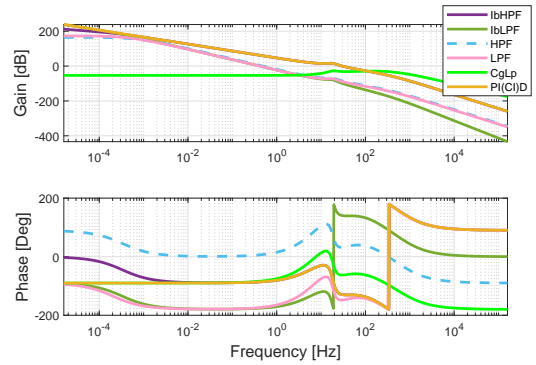


Fig. 7. 3rd order harmonics of possible reset variables of band-pass and CgLp using HOSIDFs

Figure 6 and Figure 7 show the first order harmonics and the third order harmonics of possible reset of band-pass respectively. While the gain behaviors of controllers show resemblance according to first harmonic, third harmonics of the same controllers are not alike. Also, it has been observed that phase behavior close to the bandwidth is similar to either PI²D or PI(CI)D.

IV. SYSTEM DESIGN

The implemented test setup is a simplified imitation of a 1-DOF robot based in-line metrology platform from the work of Saathof et. al. [19]. These devices require nm accuracy and they are highly sensitive to floor vibration.

Figure 5 shows the block diagram representation of the system that is used in the experiment. Base linear control (C_b) consists of PID with first order low-pass filter as in following:

$$C_b = k_p \cdot \left(1 + \frac{\omega_i}{s}\right) \cdot \left(\frac{s/\omega_d + 1}{s/\omega_t + 1}\right) \cdot \left(\frac{1}{s/\omega_f + 1}\right) \quad (12)$$

A. Experimental Setup

Setup consists of two VISATON FR10 loudspeakers (Art. no. 2020). One as a workpiece that is subjected to the floor vibrations and the other as a metrology platform. The purpose of the setup is to isolate workpiece from floor vibrations by keeping a constant distance. In this way, plant will follow the vibration source instead of attenuating the vibrations.

ADE technologies capacitive sensor is used for the experiment. It has a +/- 50 μm working range and 24 nm resolution. Dust caps of loudspeakers are replaced with 3d printed support structures so that the distance between two loudspeakers do not exceed the working range of the capacitive sensor. Sensor is mounted on the support structure of the vibration source.

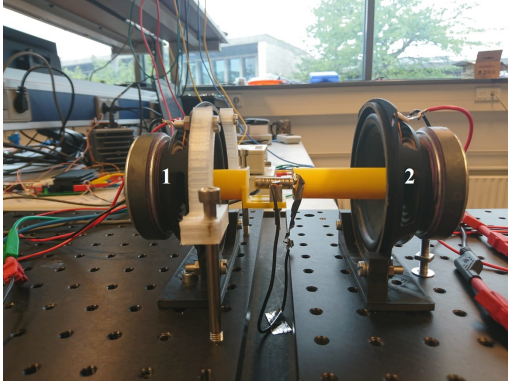


Fig. 8. Experimental Setup. (1)Vibration source , (2)Plant

CompactRIO is used together with current amplifiers for the measurement.

B. System Identification

System identification is performed for both vibration source and plant by using chirp signal. Figure 9 and Figure 10 show the frequency responses respectively

Considering the frequency response of the plant as shown in Figure 9, bandwidth is chosen as 200 Hz. Tuning parameters of the controller are shown in Table I.

Resonance frequency of the plant is observed at 45Hz. Transfer function of the plant is estimated from the System Identification Toolbox, which is found as,

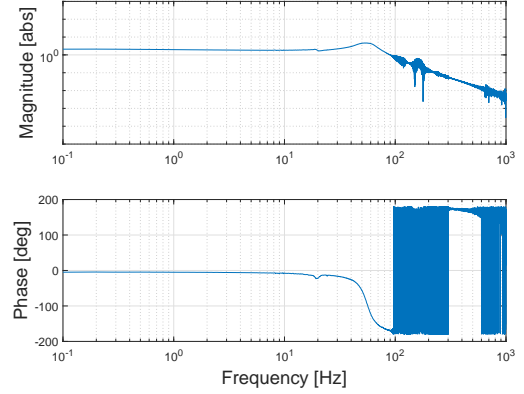


Fig. 9. Frequency response of the plant

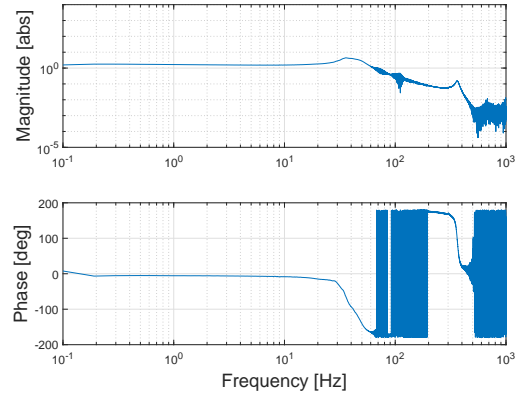


Fig. 10. Frequency response of the vibration source

Parameter	Value	Unit
k_p	2.1	
ω_i	125.6	rad/s
ω_d	418.8	rad/s
ω_t	3,769.9	rad/s
ω_f	12,566	rad/s
ω_r	2,513	rad/s

TABLE I

TUNING PARAMETERS FOR BAND-PASS CONTROLLER AND CGLP

$$P(s) = \frac{2.262e5}{s^2 + 133.7s + 1.185e5} \quad (13)$$

V. RESULTS AND DISCUSSIONS

Experiments for position locking and vibration isolation performance of the proposed methods were conducted with filtered white noise (white noise in the 0.5-30Hz frequency range), 5 Hz and 20 Hz sine wave reference inputs respectively. RMS and max error of each band-pass reset variations and CgLp are observed for the sinusoidal references and plotted in Table II. Measurement results are compared with state of the art controllers PID, PI²D, PI(CI)D respectively together with high order harmonics figures in 6 and 7 .

Measurement Results (in nm)				
	5 Hz		20 Hz	
	RMS	Max Error	RMS	Max Error
PID	788	1294	2226	3320
PI²D	147	342	1403	2148
PI(CI)D	378	1514	1315	2783
CgLp	129	342	1352	2246
IbHPF	378	1489	1310	2808
IbLPF	150	415	1398	2173
HPF	150	366	1402	2173
LPF	149	366	1402	2148

TABLE II

MEASUREMENT RESULTS IN NM. WHITE NOISE IS IN A FREQUENCY RANGE OF FLOOR VIBRATIONS(0.5-30HZ)

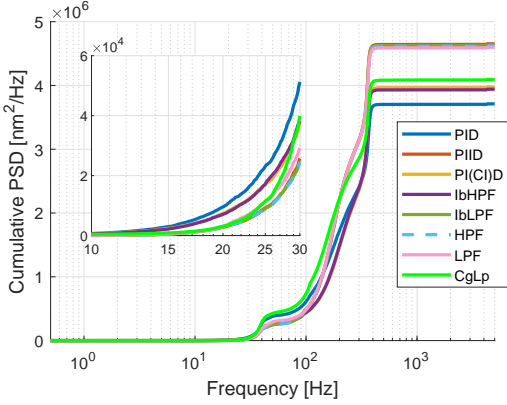


Fig. 11. Cumulative PSD starting from 0.5 Hz.

Amongst the band-pass reset variables, IbHPF gives the worst response at max error in Table II. On the other hand, the rest of the band-pass reset methods has a max error value similar to PI²D. In Figure 7, higher order harmonics of IbLPF, HPF and LPF shows same gain behavior at 5 and 20 Hz, and their gain are lower than IbHPF. Because of the high higher order harmonics, IbHPF gives poor max error response. In measurement with 5 Hz sine wave input, CgLp has the best Max RMS value, 129 nm, an improvement around 12%. Although CgLp has a similar high order harmonic response than the band-pass reset approaches IbLPF, HPF and LPF at 5 Hz, It reaches a better result due to the higher phase margin. On the other hand, measurement results with 20 Hz sine wave input shows that CgLp has worse response than IbLPF, HPF, LPF. The reason of worse results is the presence of high order harmonics shown in Figure 7.

To check the performance of the proposed controllers in the region of interest, the cumulative PSDs (CPSD) of error from white noise measurements is plotted in Figure 11. CPSDs are plotted from the starting frequency of floor vibrations, 0.5 Hz. PI(CI)D and IbHPF showed similar responses. On the other hand, PI²D, IbLPF, HPF and LPF have the similar CPSD response although their open loop frequency behavior in terms of high harmonics was not identical.

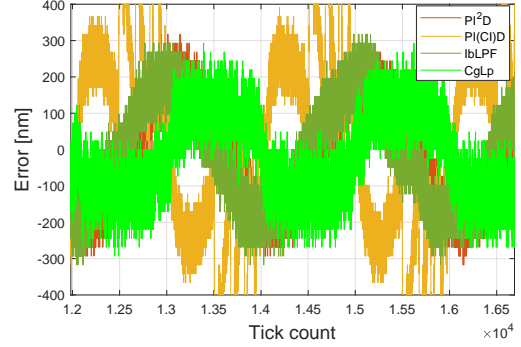


Fig. 12. 5 Hz sinusoidal input disturbance responses of closed loop systems

VI. CONCLUSIONS

Floor vibrations are a common problem in precision instruments, such as wafer scanners and metrology applications, where high accuracy and accelerations are needed for high performance. Due to the limitations of linear control, research has been done in improving reset control performance for vibration isolation. While reset control gives improvement in phase margin, it introduces unwanted dynamics into the system due to the high order harmonics.

This paper presented the investigation on improving reset control performance by attenuating high-order harmonics. The proposed band-pass controller is focused on improving the overall performance by implementing reset only within the frequency region of floor vibrations. Phase compensation through CgLp filter is also looked into as a different strategy to achieve the same.

The proposed controller is implemented on a setup, a simplified imitation of a 1-DOF robot based in-line metrology platform, where the plant follows the vibration source instead of attenuating it. Experimental results showed, IbLPF, HPF and LPF were able to improve disturbance rejection (DR) performance as good as of PI²D. CgLp has been tested in [18] for improved tracking performance along with the use of a feedforward control, feedforward cannot be used in the case of disturbance rejection. However, CgLp still shows significantly improved performance compared to state of the art.

Based on the findings, one can conclude applying reset

control for CgLp will increase the system performance of high-tech instruments. CgLp made it possible to reach disturbance rejection performance PI^2D while having phase characteristics of $PI(CI)D$. Further, smart application of reset can ensure improved performance and ensure that the demands of the high tech industry can be met.

REFERENCES

- [1] I. Fujita, F. M. Sakai, and S. Uzawa, "Next-generation scanner to sub-100-nm lithography," in *Optical Microlithography XVI*, vol. 5040. International Society for Optics and Photonics, 2003, pp. 811–822.
- [2] S. Ryan, "Optical table advances quiet vibrations in highly sensitive applications," *LASER FOCUS WORLD*, vol. 53, no. 9, pp. 27–30, 2017.
- [3] D. A. H. Laro, "Mechatronic design of an electromagnetically levitated linear positioning system using novel multi-dof actuators," Ph.D. dissertation, TU Delft, Delft University of Technology, 2009.
- [4] K. J. Astrom and T. Hagglund, "The future of PID control," *Control Engineering Practice*, vol. 9, no. 11, pp. 1163–1175, 2001.
- [5] J. Mao, H. Tachikawa, and A. Shimokohbe, "Double-integrator control for precision positioning in the presence of friction," *Precision engineering*, vol. 27, no. 4, pp. 419–428, 2003.
- [6] R. M. Schmidt, G. Schitter, and A. Rankers, *The Design of High Performance Mechatronics-: High-Tech Functionality by Multidisciplinary System Integration*. IOS Press, 2014.
- [7] J. C. Clegg, "A nonlinear integrator for servomechanisms," *Transactions of the American Institute of Electrical Engineers, Part II: Applications and Industry*, vol. 77, no. 1, pp. 41–42, 1958. [Online]. Available: <http://ieeexplore.ieee.org/document/6367399/>
- [8] Y. Li, G. Guo, and Y. Wang, "Reset control for midfrequency narrow-band disturbance rejection with an application in hard disk drives," *IEEE Transactions on Control Systems Technology*, vol. 19, no. 6, pp. 1339–1348, 2011.
- [9] A. Banos and A. Vidal, "Design of Reset Control Systems: The PI + CI Compensator," *Journal of Dynamic Systems, Measurement, and Control*, vol. 134, no. 5, p. 051003, 2012. [Online]. Available: <http://dynamicsystems.asmedigitalcollection.asme.org/article.aspx?articleid=1478002>
- [10] A. Vidal and A. Banos, "Stability of reset control systems with variable reset: Application to pi+ ci compensation," in *Control Conference (ECC), 2009 European*. IEEE, 2009, pp. 4871–4876.
- [11] —, "QFT-based design of PI+ CI reset compensators: application in process control," *Control and Automation, 2008 16th ...*, pp. 806–811, 2008. [Online]. Available: http://ieeexplore.ieee.org/xpls/abs/_all.jsp?arnumber=4602123
- [12] J. Zheng, Y. Guo, M. Fu, Y. Wang, and L. Xie, "Improved reset control design for a pzt positioning stage," in *Control Applications, 2007. CCA 2007. IEEE International Conference on*. IEEE, 2007, pp. 1272–1277.
- [13] A. Baños and A. Barreiro, *Reset Control Systems*, ser. Advances in Industrial Control. London: Springer London, 2012. [Online]. Available: <http://www.springer.com/engineering/control/book/978-0-85729-634-4http://link.springer.com/10.1007/978-1-4471-2250-0>
- [14] W. E. Vander Velde, *Multiple-input describing functions and nonlinear system design*. McGraw-Hill, New York, 1968.
- [15] Y. Guo, Y. Wang, and L. Xie, "Frequency-domain properties of reset systems with application in hard-disk-drive systems," *IEEE Transactions on Control Systems Technology*, vol. 17, no. 6, pp. 1446–1453, 2009.
- [16] P. Nuij, O. Bosgra, and M. Steinbuch, "Higher-order sinusoidal input describing functions for the analysis of non-linear systems with harmonic responses," *Mechanical Systems and Signal Processing*, vol. 20, no. 8, pp. 1883 – 1904, 2006. [Online]. Available: <http://www.sciencedirect.com/science/article/pii/S088832700500083X>
- [17] K. Heinen, "Frequency analysis of reset systems ." [Online]. Available: <http://www.sciencedirect.com/science/article/pii/S088832700500083X>
- [18] N. Saikumar, R. K. Sinha, and S. H. HosseinNia, "'constant in gain lead in phase' element - application in precision motion control," 2018.
- [19] R. Saathof, M. Thier, R. Hainisch, and G. Schitter, "Integrated system and control design of a one dof nano-metrology platform," *Mechatronics*, vol. 47, pp. 88–96, 2017.

Chapter 5

Conclusion

In this thesis, disturbance rejection of reset systems against floor vibrations is discussed. Reset strategies are investigated regarding phase reduction and phase compensation. Based on the literature review paper, the gap in the area regarding disturbance rejection performance as well as the negative effects of high-order harmonics are pointed out. Based on these conclusions, the band-pass reset control is proposed. The proposed controller is aimed to attenuate high-order harmonics. Following are the main contributions of this research:

- Based on the measurement result, one can conclude that CgLp achieves better vibration isolation performance than PI(CI)D against the region of interest (0.5-30 Hz), while keeps the phase characteristics of PI(CI)D.
- Comparing the measurement results of the band-pass controller with CgLp, it is evident that phase compensation with reset (CgLp method) gives better performance compared to band-pass control, where reset creates phase reduction. Based on these findings, one can conclude that it is more beneficial to apply reset within the bandwidth region than the frequency region of floor vibrations (0.5-30 Hz).
- It has been showed in the literature that CgLp works well with feedforward on removing negative effects of high-order harmonics without degrading the reset performance [7]. However, based on this particular setup, measurements showed that good performance could be achieved without the presence of feed-forward control as well.

Appendix A

Loop Shaping

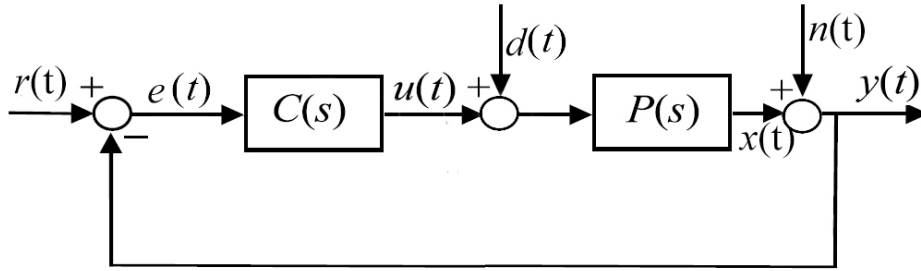


Figure A-1: A closed loop control system with process and output disturbance

Loop Shaping plays a powerful role for designing a closed loop system by tuning the open loop transfer function such that it meets the design objectives in terms of stability, performance and robustness. A feedback controlled system is given in Figure A-1, where $d(t), n(t), y(t), e(t), u(t), r(t)$ and $x(t)$ denote process disturbance, output disturbance, system output, control input, control output, reference input and output of the plant respectively. Open loop is described as $L(s) = C(s)P(s)$ where $C(s)$ and $P(s)$ denote controller and plant respectively. Although required design objectives are conflicting in nature, most of them can be met by shaping $L(s)$ in such way that it has a large loop gain at low frequencies below crossover, and a low gain at high frequencies above crossover. The reasoning behind this can be explained by looking at the real error in Figure A-1.

$$e_{real} = y - x = \frac{1}{1+L}r - \frac{G}{1+L}d + \frac{L}{1+L}n \quad (\text{A-1})$$

$$= \mathbf{S}r - \mathbf{P}\mathbf{S}d + \mathbf{T}n \quad (\text{A-2})$$

In Equation A-2, \mathbf{S} denotes sensitivity function that gives information about disturbance rejection performance of a closed loop system that appears on the output. It is desired to

have low \mathbf{S} below the bandwidth and high \mathbf{S} above the bandwidth. Because, high \mathbf{S} indicates better noise rejection. Whereas, low \mathbf{S} means better tracking, meaning high control gain.

\mathbf{T} , Complementary sensitivity function, tells us how well the system output can follow the reference input. Closer to 1, better following a prescribed path trajectory. In linear controllers \mathbf{T} and \mathbf{S} add to unity. This cause a limitation on linear controllers known as waterbed effect.

Finally, \mathbf{PS} , process sensitivity function, shows the effect of disturbance in output. PS is the ratio of output $y(t)$ to process disturbance $d(t)$ where $d(t)$ and $y(t)$ are shown in Figure A-1 [8]. Lower PS means higher ability to reject disturbances. Since changing the plant is not an option, the only possible solution is to change the controller to have increased disturbance rejection performance. From PS formula, It is clear that the controller gain must be increased to have higher disturbance rejection.

Appendix B

Loudspeaker Datasheet

10 cm Breitbandlautsprecher / 4" Fullrange Speakers

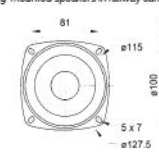
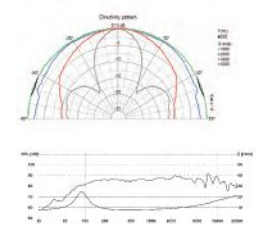
Art. No. 2020 – 4 Ω Art. No. 2021 – 8 Ω FR 10

10 cm (4") Breitbandlautsprecher mit guten Tieftoneigenschaften, ausgeglichenem Frequenzgang und hohem Wirkungsgrad. Besonders geeignet als Einbaulautsprecher für die Musikwiedergabe sowie zur Bestückung von ELA-Zeilen. **Zubehör:** Schutzgitter (Art. No. 4642, 4640, 4670, 4744)

Anwendungsmöglichkeiten: ELA-Zeilen, Deckenlautsprecher in Schienenfahrzeugen und Bussen, Car-HiFi Einbaulautsprecher, Elektronische Musikinstrumente

10 cm (4") fullrange speaker with good bass reproduction, balanced frequency response and high efficiency. Especially suitable as built-in speaker for music reproduction and as driver for 100 V network column speakers. **Accessories:** Protective grille (Art. No. 4642, 4640, 4670, 4744)

Typical applications: Network column speakers, Ceiling-mounted speakers in railway carriages and busses, Built-in car hi-fi speakers, Electronic musical instruments



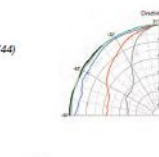
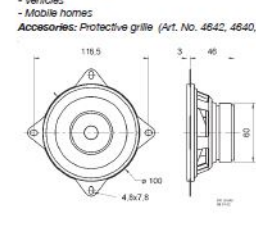
Art. No. 4640
Art. No. 4642
Art. No. 4744 Art. No. 4670

Industrie / Industry

Art. No. 4898 – 4 Ω Art. No. 4899 – 8 Ω FR 10 HM

10 cm (4") Breitbandlautsprecher mit Hochtonkegel und Euro-Normkorb. Einfache Montage in Fahrzeugen mit Einbaufürten für 10-cm-Lautsprecher. **Anwendungsmöglichkeiten:** - Fahrzeuge - Reisemobile **Zubehör:** Schutzgitter (Art. No. 4642, 4640, 4744)

10 cm (4") fullrange speaker with tweeter cone and European standard basket. Simple fitting in vehicles with cut-outs for 10 cm speakers. **Typical applications:** - Vehicles - Mobile homes **Accessories:** Protective grille (Art. No. 4642, 4640, 4744)



Art. No. 4640
Art. No. 4642
Art. No. 4744

Industrie / Industry

		FR 10	FR 10 HM
Nenn-/Musikbelastbarkeit	Rated/maximum power	30 W / 50 W	20 W / 30 W
Impedanz	Impedance	4 Ω/8 Ω	4 Ω/8 Ω
Übertragungsbereich (-10 dB)	Frequency response (-10 dB)	60-20000 Hz	65-20000 Hz
Mittlerer Schalldruckpegel	Mean sound pressure level	86 dB (1 W/1 m)	86 dB (1 W/1 m)
Chromatentieftiefe	Excursion limit	± 4 mm	± 2 mm
Resonanzfrequenz	Resonance frequency	90 Hz/98 Hz	120 Hz
Obere Polsterentiefe	Height of front pole-piece	3 mm	2 mm
Schwebescheibendurchmesser	Voice coil diameter	20 mm Ø	14 mm Ø
Wickelhöhe	Height of winding	8 mm	5 mm
Schwebescheibendurchmesser	Cutout diameter	100 mm Ø	94 mm Ø
Gewicht netto	Net weight	0,58 kg	0,34 kg

Webseite Daten: 156-157 / for further data see pages 156-157

VISATON Lieferprogramm / Main Catalogue 2009/2010 29

Detailed Setup Description

C-1 General Requirements

The focus of this research is primarily on the controller. To validate the system responses, a simple setup is more advantageous, since there will be less complications. Therefore, 1-DoF mechatronic system design is sufficient for reference tracking and to prove the concept of the designed controller.

Intended setup has to be an imitation of a high precision system. For this reason, high acceleration and velocity are desired. Working range of the demonstrator should be in micrometer levels. Therefore, a sensor with high resolution, accuracy and precision is needed.

It is mentioned in the paper that floor vibrations are present in a frequency range between 0.5-30 Hz. The desired setup is intended to follow the floor vibrations. Which means, given frequency range is required to be below the resonance frequency of the plant. So that the plant can follow the floor vibrations.

Taking aforementioned requirements into consideration, the chosen experiment setup is a simplified imitation of a 1-DOF robot based in-line metrology platform from the literature [9]. Industrial robot arms have a micrometer accuracy. However, AFM that is mounted on robot arm requires nm accuracy and is very sensitive to floor vibrations. The idea here is that, instead of isolating workpiece and AFM from floor vibrations, the metrology platform keeps a constant distance between workpiece and AFM, using controller. For simplicity, only the fine stage is considered.

C-2 Conceptual Design

Conceptual design consists of 2 loudspeakers. They are represented as single-mass-damper system in Figure C-1. One loudspeaker is used as a vibration source. Whereas, the other will represent the metrology platform. Sensor is placed between the loudspeakers to keep track of the distance. This way metrology platform can follow the vibration source.

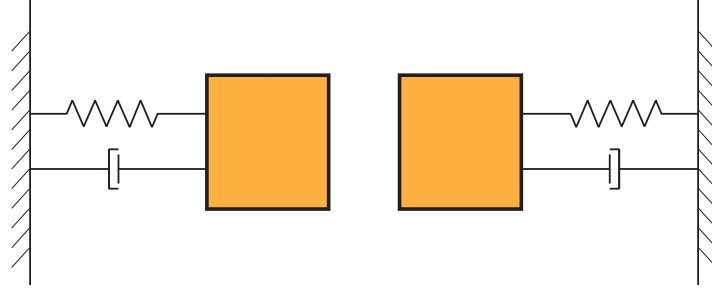


Figure C-1: Conceptual design of the setup.

Working principle of a loudspeaker is simple. First, an electric signal is created and transmitted to the voice coil. Voice coil uses this electric signal and converts it to a force. Diaphragm, which is connected to the coil moves and radiates sound by the incoming force. It can be calculated analytically by using the following equation:

$$F = Bli \quad (\text{C-1})$$

where B , l , i denote magnetic field strength, length of the coil and the current flowing through the coil respectively. Before introducing the final design, the following concepts were considered.

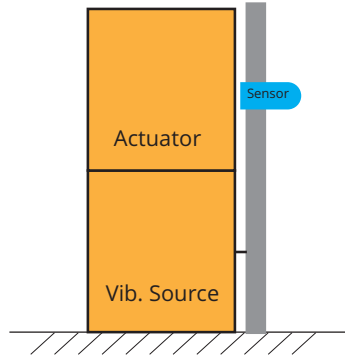


Figure C-2: Design concept no.1

In the first design concept, shown in Figure C-2, actuator is placed on top of the vibration source. A leaf spring, shown as gray rectangle, is placed in front loudspeaker. Sensor, shown as blue, is connected to the leaf spring. Whereas, leaf spring is attached to the cone of the loudspeaker (vibration source). The movement of the vibration source will be transmitted to the leaf spring. Sensor will read the relative distance between the actuator and the leaf spring. Then, actuator will start to follow the movement of the leaf spring according to the sensor data. This simple design concept is not chosen because vibration that is caused by the loudspeakers would be transmitted to each other directly and affect the system performance.

In the next design concept, Figure C-3, actuator and vibration sources are placed in front of each other on the same ground. Leaf springs are connected to the loudspeakers cones. Sensor is placed same as the design concept no.1. Sensor will read the distance of the leaf spring

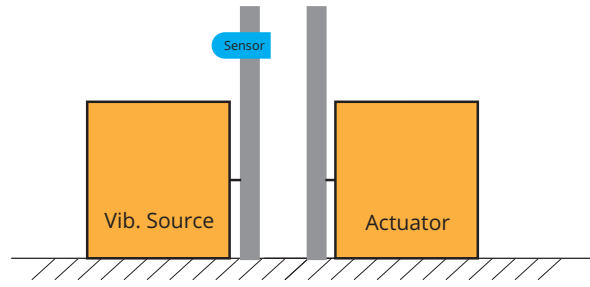


Figure C-3: Design concept no.2

and the actuator would move to keep the same distance. In this concept, vibrations that are caused by the actuators would still be transmitted to each other from the ground. Also, parasitic motions caused by the leaf springs would be observed at high displacements as well. As a result, final design concept shown in Figure C-4 is adopted.

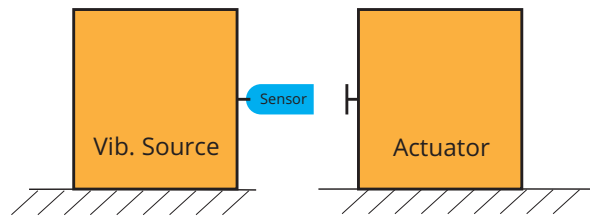


Figure C-4: Chosen design concept

In the chosen concept, leaf springs are removed. Sensor is placed on a interface which is directly attached to the cone. Unlike leaf springs, sensor here would not measure the displacement that is caused by bending. Instead, sensor would measure the relative distance between the actuators directly. In that way, possible parasitic motions that would be caused by leaf springs are eliminated. Finally, loudspeakers are placed on two separate vibration isolation tables in order to reduce the vibrations that would come from the movement of the other loudspeaker. Drawback of the chosen concept is the alignment. One must be extra careful aligning the places of loudspeakers and the position of the sensor.

C-3 Detailed Setup

Finalized setup consists of two VISATON FR10 loudspeakers (Art. no. 2020) due to it's high working range and resonance frequency above the frequency range of floor vibrations. More importantly, loudspeakers can be controlled with high accuracy due to the low parasitic forces. They have low moving mass, which makes it possible to reach high accelerations. Since they use voice coil actuators, their force to current relation is linear. However, loudspeakers give nonlinear behavior at frequencies. Nonlinear effect can be decreased as input value decreases.

Capacitive sensor is used for tracking relative distance. It has a $\pm 50\mu\text{m}$ working range and 24 nm resolution. This type of sensor is chosen because capacitive sensors have high accuracy, precision and resolution values which fits the general requirements of the setup. The only trade-off is the low working range. However, this problem is fixed after the mechanical

structure of the setup. The structure of the chosen concept is built in solidworks as shown in Figure C-5.

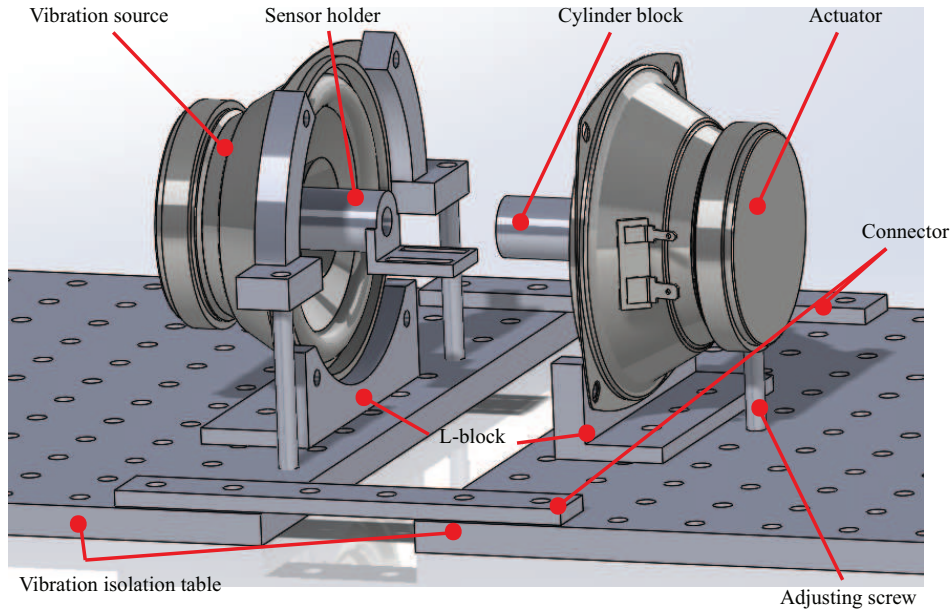


Figure C-5: Solidworks model of the finalized concept

To prevent the parasitic motions, loudspeakers should be placed rigidly. Therefore, loudspeakers are connected to L-blocks which are fixed to the isolation table. Additional structures are built and attached to the loudspeaker to ensure high stiffness. Capacitive sensor is placed on the sensor holder. Due to the small working range of the sensor, cylinder block is attached to the cone of the actuator, so that sensor can work properly. The blocks that are attached to the cone increases the moving mass which decreases the resonance frequency of the actuators. However, it is validated from the system identification that the new natural frequency of the actuators are still higher than the frequency range of floor vibrations. Adjusting screw is used to do fine tuning of the positioning of the sensor. Finally, connectors are used for aligning the isolation tables. They are removed after alignment.

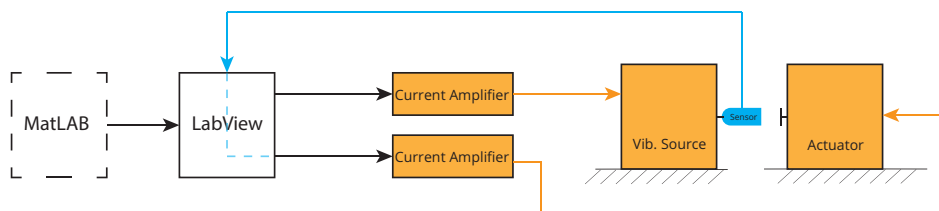


Figure C-6: Schematic overview of the experiment setup

LabView real time control is used to read out the position measurement from the capacitive sensor and to send the electric signal. Electric signals are amplified in the current amplifiers and goes to loudspeakers. MatLAB is used to convert continuous transfer function into

discrete function.

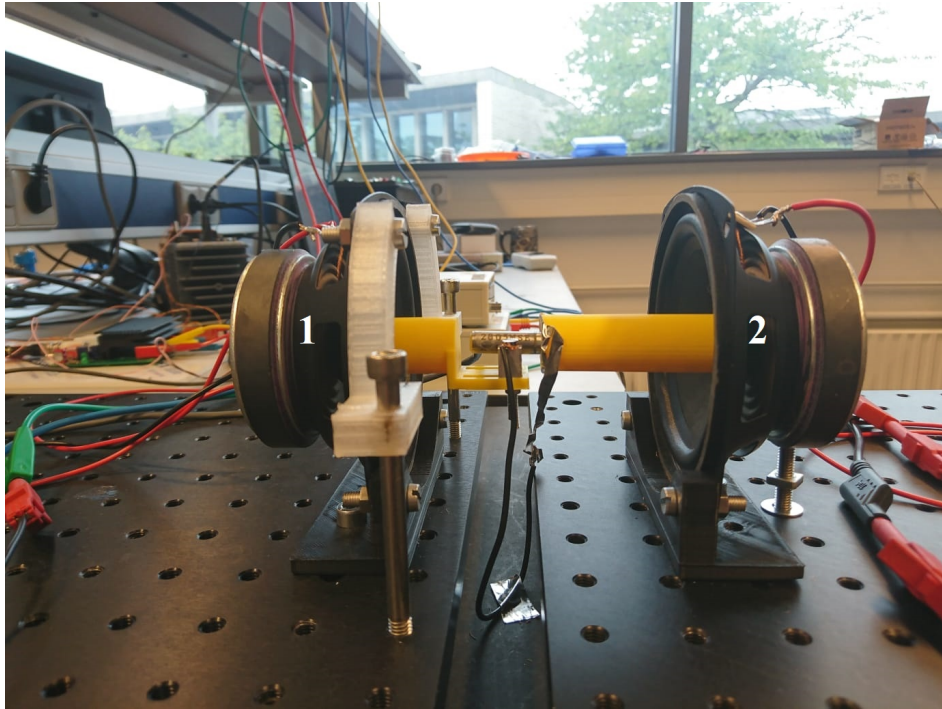


Figure C-7: Finalized setup. 1) Vibration source, 2) Actuator

BandPass Reset Control Analysis

The idea of creating band-pass reset control revolves around reducing the negative effect of high order harmonics in the system. As mentioned in the paper, floor vibrations are present at low frequencies. Using reset element in a complete frequency range, like Clegg Integrator, might increase the overall performance depending on your system. However, it is inevitable that high order harmonics will be introduced into the system, affecting the max error of overall performance negatively by causing spikes in the control output as shown in ???. Because of this reason, work is investigated on ways to decrease the unwanted effects of high order harmonics. Possible solution is to introduce reset only within the frequency range of floor vibrations. In the next section, two novel approaches are investigated.

D-1 HPF-LPF Option

Band-pass reset action in this approach is created by the help of a high-pass filter and a low-pass filter. Consider they have same cut-off frequency, ω_c . Their transfer functions are:

$$HPF = \frac{s}{\omega_c + s} \qquad LPF = \frac{\omega_c}{\omega_c + s} \qquad (D-1)$$

If a linear integrator ($1/s$) is introduced before these filters, then the result will be a linear integrator as shown in the following equation.

$$HPF + LPF = 1 \qquad (D-2)$$

$$\frac{1}{s}.HPF + \frac{1}{s}.LPF = \frac{1}{s} \qquad (D-3)$$

This gives 4 possible variables to reset. Clegg integrator can be formed if both integrators are reset. However, reset action can be introduced before or after the ω_c , if only one of the

integrator is reset as can be seen from Figure D-1. It is important to note that resetting one of the integrator decreases gain around the cut-off frequency. Therefore, it is important to take this effect into considering before choosing the cut-off frequency.

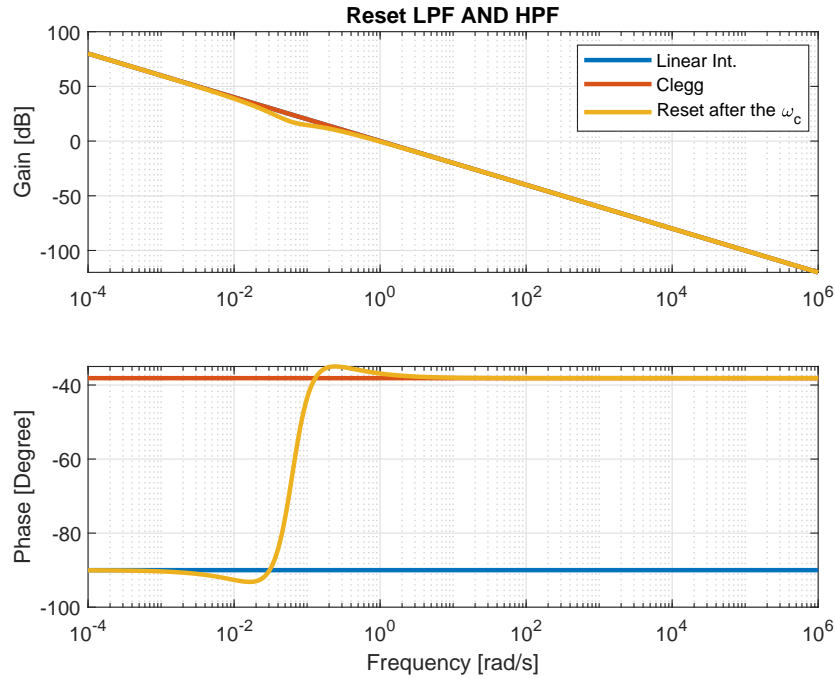


Figure D-1: Comparison between HPF-LPF option and state of the art controllers

Figure D-1 shows frequency response of resetting integrator before the HPF. HPF filters the signal before its cut-off frequency. Therefore, reset action is only visible after it. There are several cases of using reset. Some of them are:

- Resetting Integrator before the HPF (IbHPF)
- Resetting Integrator before the LPF (IbLPF)
- Resetting Integrator AND HPF (IaHPF)
- Resetting Integrator AND LPF (IaLPF)
- Resetting only HPF (HPFonly)
- Resetting only LPF (LPFonly)

and so on... To determine the best case, following factors were examined:

1. Effect of high-order harmonics: lower the higher order harmonics, better the overall performance.

2. Phase Margin: By definition, phase margin is the difference between the phase lag and -180 at the bandwidth frequency. High phase margin indicates a more robust performance, which is desired.
3. Phase in BW region.
4. Phase in the region of interest.

Following plots show the 1st, 3rd and 5th order harmonics of various cases.

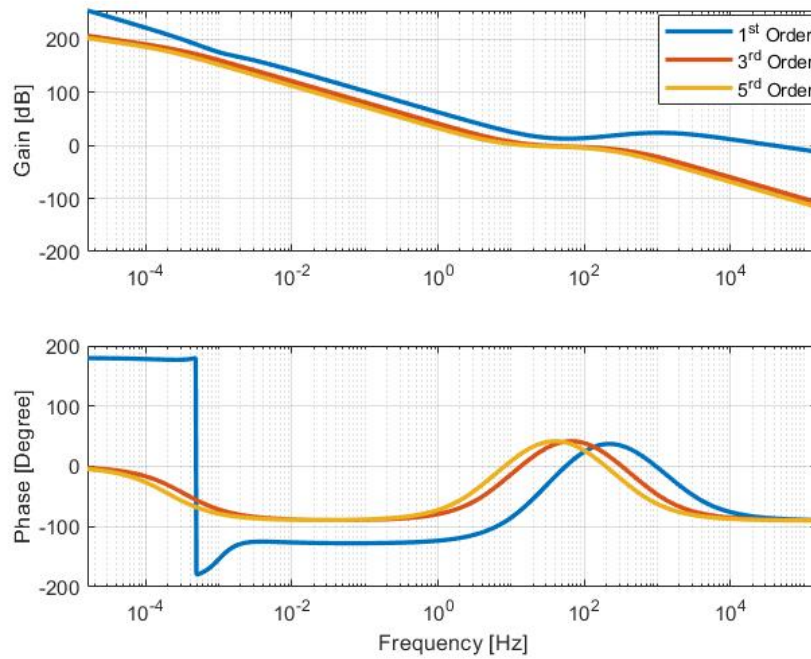


Figure D-2: Case IbHPF

Considering high order harmonics plot, it is expected that IbHPF and IaLPF should give the best response. Since, their effect of high order harmonics is less significant.

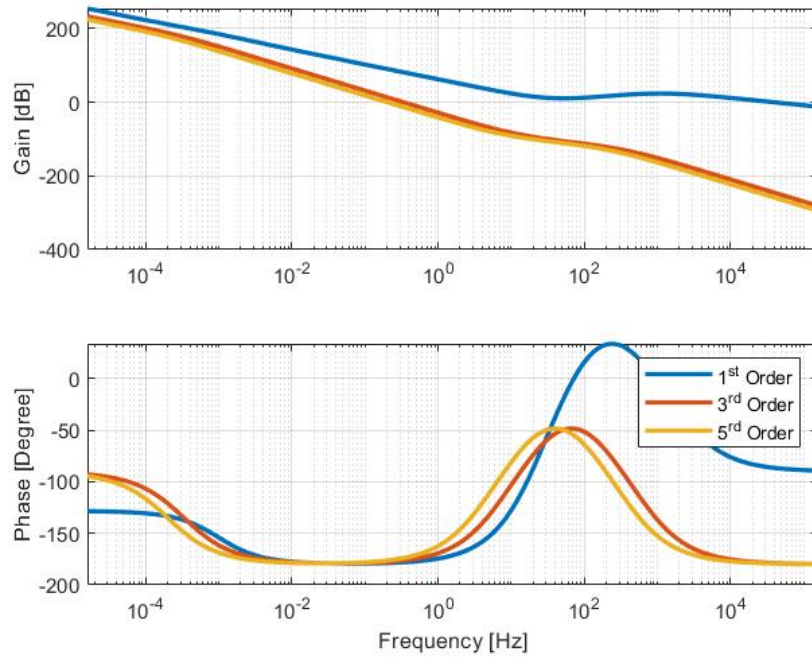


Figure D-3: Case lbLPF

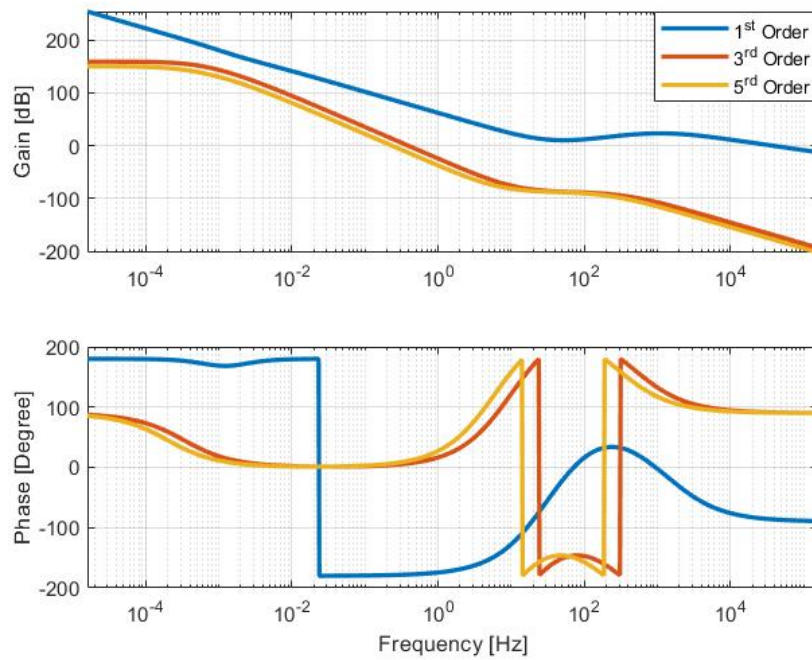


Figure D-4: Case HPFonly

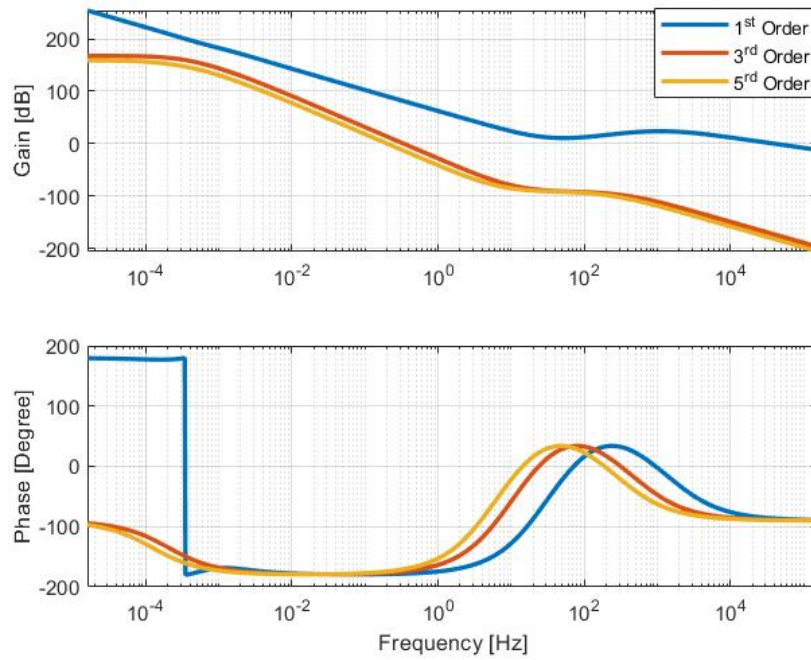


Figure D-5: Case LPFonly

Appendix E

Current Amplifier V/A Ratio

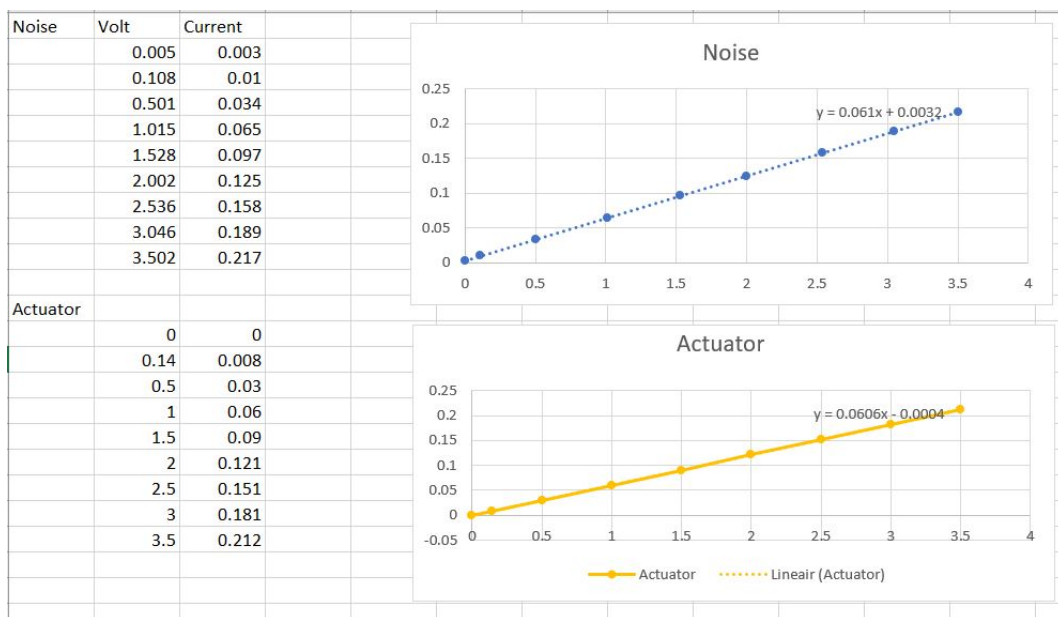


Figure E-1: Current Amplification rates

Bibliography

- [1] I. Fujita, F. M. Sakai, and S. Uzawa, "Next-generation scanner to sub-100-nm lithography," in *Optical Microlithography XVI*, vol. 5040, pp. 811–822, International Society for Optics and Photonics, 2003.
- [2] S. Ryan, "Optical table advances quiet vibrations in highly sensitive applications," *LASER FOCUS WORLD*, vol. 53, no. 9, pp. 27–30, 2017.
- [3] D. A. H. Laro, *Mechatronic design of an electromagnetically levitated linear positioning system using novel multi-DoF actuators*. PhD thesis, TU Delft, Delft University of Technology, 2009.
- [4] K. J. Astrom and T. Hagglund, "The future of PID control," *Control Engineering Practice*, vol. 9, no. 11, pp. 1163–1175, 2001.
- [5] J. Mao, H. Tachikawa, and A. Shimokohbe, "Double-integrator control for precision positioning in the presence of friction," *Precision engineering*, vol. 27, no. 4, pp. 419–428, 2003.
- [6] O. Beker, C. V. Hollot, Y. Chait, and H. Han, "Fundamental properties of reset control systems," *IFAC Proceedings Volumes (IFAC-PapersOnline)*, vol. 15, no. 1, pp. 187–192, 2002.
- [7] N. Saikumar, R. K. Sinha, and S. H. HosseinNia, "'constant in gain lead in phase' element - application in precision motion control," 2018.
- [8] R. M. Schmidt, G. Schitter, and A. Rankers, *The Design of High Performance Mechatronics-: High-Tech Functionality by Multidisciplinary System Integration*. IOS Press, 2014.
- [9] R. Saathof, M. Thier, R. Hainisch, and G. Schitter, "Integrated system and control design of a one dof nano-metrology platform," *Mechatronics*, vol. 47, pp. 88–96, 2017.